ANALYSIS AND PERFORMANCE MEASUREMENTS OF MIMO OFDM TECHNIQUES FOR LTE

İSMAİL İBİŞOĞLU

JANUARY 2018

ANALYSIS AND PERFORMANCE MEASUREMENTS OF MIMO OFDM TECHNIQUES FOR LTE

A THESIS SUBMITTED TO

THE GRADUATE SCHOOL OF NATURAL AND APPLIED

SCIENCES OF

ÇANKAYA UNIVERSITY

BY

İSMAİL İBİŞOĞLU

IN PARTIAL FULFILLMENT OF THE REQUIREMENTS FOR THE

DEGREE OF

MASTER OF SCIENCE

IN

THE DEPARTMENT OF

ELECTRONIC AND COMMUNICATION ENGINEERING

JANUARY 2018

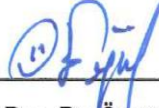Title of the Thesis: **Analysis and performance measurements of MIMO OFDM techniques for LTE.**

Submitted by **İsmail İBİŞOĞLU**

Approval of the Graduate School of Natural and Applied Sciences, Çankaya University.

Prof.Dr. Can ÇOĞUN
Director

I certify that this thesis satisfies all the requirements as a thesis for the degree of Master of Science.

Yrd. Doç. Dr. Özgür ERGÜL
Head of Department (v)

This is to certify that we have read this thesis and that in our opinion it is fully adequate, in scope and quality, as a thesis for the degree of Master of Science.

Prof. Dr. Halil Tanyer EYYUBOĞLU
Supervisor

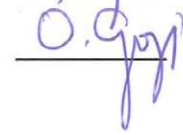**Examination Date: 19.01.2018**

Examining Committee Members

Assoc. Prof. Dr. Fırat HARDALAÇ	(Gazi Univ.)	
Prof. Dr. Halil Tanyer EYYUBOĞLU	(Çankaya Univ.)	
Assoc. Prof. Dr. Orhan GAZİ	(Çankaya Univ.)	

STATEMENT OF NON-PLAGIARISM PAGE

I hereby declare that all information in this document has been obtained and presented in accordance with academic rules and ethical conduct. I also declare that, as required by these rules and conduct, I have fully cited and referenced all material and results that are not original to this work.

Name, Last Name : İsmail İBİŞOĞLU

Signature :

Date : 19.01.2018

ABSTRACT

ANALYSIS AND PERFORMANCE MEASUREMENTS OF MIMO OFDM TECHNIQUES FOR LTE

İBİŞOĞLU, İsmail

M.Sc., Department of Electronic and Communication Engineering

Supervisor: Prof. Dr. Halil Tanyer EYYUBOĞLU

January 2018, 82 pages

Nowadays, the demand towards mobile phones that require high data rates applications has rapidly increased. In mobile networks, the Third Generation Partnership Project (3GPP) to meet the increasing demand developed long-term evolution (LTE) standard. Today, on February 28th, 2017[1], 790 operators have commercially launched LTE in 201 countries, according to data released this week by GSA (Global mobile Suppliers Association) in its latest update of the Evolution to LTE report.

This study has analyzed LTE network structure which is based 3GPP standards, Version 7, 8, 9, 10, 11 and 12, and defined LTE technology properties. Afterwards, information is offered about different methods for capacity and coverage area calculations. This study also tested whether Shannon Capacity Equality or using software (like ATOLL) tools are preferred by today operators on sample.

Keywords: LTE, Coverage, Capacity, Frequency Planning, ATOLL Radio Network Planning &Optimisation

ÖZ

LTE İÇİN MIMO OFDM TEKNİKLERİNİN İNCELENMESİ VE PERFORMANS ÖLÇÜMLERİ

İBİŞOĞLU, İsmail

Yüksek Lisans, Elektronik ve Haberleşme Mühendisliği Anabilim Dalı

Tez Yöneticisi: Prof. Dr. Halil Tanyer EYYUBOĞLU

Ocak 2018, 82 sayfa

Günümüzde cep telefonları üzerinden yüksek veri hızları gerektiren uygulamalara olan talep hızla artmıştır. Mobil şebekelerde, artan talebi karşılamak üzere 3. Nesil Ortaklık Projesi (3GPP) tarafından uzun vadeli evrim (LTE) standartları geliştirilmiştir. Bugün, 28 Şubat 2017' de evrimin en son güncellenmesinde GSA tarafından bu hafta veri bırakılmasına göre LTE raporu 790 işletmeciler 201 ülkede ticari lansmana sahip[1].

Bu çalışmada, LTE network yapısı incelenmiştir. 3 GPP Versiyon 7, 8, 9, 10, 11 ve 12 standartları esas alınarak LTE teknoloji özelliklerin tanımlaması yapılmıştır. Daha sonra, kapasite ve kapsama alanı hesaplamaları için değişik metotlardan hakkında bilgi verilmiştir. Aynı zamanda, örnek üzerinden gerek Shannon kapasite eşitliği gerek ise günümüz operatörleri tarafından kullanılan yazılımlar (Atoll) araçları kullanılarak yapılmıştır.

Anahtar Kelimeler: LTE, Kapsama, Kaplama, Frekans Planlama, ATOLL Radyo Network Planlama ve Optimizasyon

ACKNOWLEDGEMENTS

I would like to express my sincere gratitude to Prof. Dr. Halil Tanyer EYYUBOĞLU for his supervision, special guidance, suggestions, and encouragement through the development of this thesis.

It is a pleasure to express my special thanks to my family for their valuable support.

TABLE OF CONTENTS

CHAPTERS:

LIST OF ABBREVIATIONS

3GPP	3rd Generation Partnership Project
4G	4th Generation
ACLR	Adjacent Channel Leakage Ratio
AMC	Adaptive Modulation and Coding
AWGN	Additive White Gaussian Noise
BCH	Broadcast Channel
BER	Bit Error Rate
BH	Busy Hour
BLER	Block Error Rate
CCU	Cell Center User
CDMA	Code Division Multiple Access
CEU	Cell Edge User
CP	Cyclic Prefix
CQI	Channel Quality Indicator
CSI	Channel State Information
DFT	Discrete Fourier Transform
DLSCH	Downlink Shared Channel
DRS	Demodulation Reference Signal
EDGE	Enhanced Data Rates for GSM Evolution
EUTRA	Evolved UMTS Terrestrial Radio Access
E-UTRAN	Evolved UMTS Terrestrial Radio Access Network
FDD	Frequency Division Duplex
FDMA	Frequency Division Multiple Access
FFT	Fast Fourier Transform
FRF	Frequency Reuse Factor
GSA	Global mobile Suppliers Association
GSM	Global System for Mobile Communication

HSPA	High Speed Packet Access
ICI	Inter Carrier Interference
IFFT	Inverse Fast Fourier Transform
ISI	Inter Symbol Interference
LTE	Long Term Evolution
MAC	Medium Access Control
MCS	Modulation and Coding Scheme
MIB	Master Information Block
MIMO	Multiple Input Multiple Output
MU-MIMO	Multi User MIMO
OFDM	Orthogonal Frequency-Division Multiplexing
OFDMA	Orthogonal Frequency-Division Multiple Access
PAPR	Peak-to-Average Power Ratio
PBCH	Physical Broadcast Channel
PL	Path Loss
PRACH	Physical Random Access Channel
PSS	Primary Synchronization Signal
PSK	Phase-Shift Keying
PUCCH	Physical Uplink Control Channel
PUSCH	Physical Uplink Shared Channel
QAM	Quadrature Amplitude Modulation
QPSK	Quadrature Phase Shift Keying
RB	Resource Block
REFSENS	Reference Sensitivity
RF	Radio Frequency
SC-FDMA	Single-Carrier Frequency-Division Multiple Access
SFR	Soft Frequency Reuse
SIB	System Information Block
SIR	Signal to Interference
SL	System Loss
SINR	Signal to Interference and Noise Ratio
SNR	Signal to Noise Ratio
SRS	Sounding Reference Signal

SSS	Secondary Synchronization Signal
SU-MIMO	Single User MIMO
TBS	Transport Block Size
TDD	Time Division Duplex
TDMA	Time Division Multiple Access
TTI	Transmission Time Interval
UE	User Equipment
UMTS	Universal Mobile Telecommunications System
WCDMA	Wideband Code Division Multiple Access

CHAPTER 1

1. INTRODUCTION

1.1. Background

Tondare S. M., Panchal S. D. and Kushnure D. T. offer information about the properties of 1G, 2G,3G,4G and 5G mobile networks and the technology as well as comparing them [2].

Gilberto Berardinelli, Luis Angel, Simone Frattasi, etc. argue the convenience of using OFDMA or SC-FDMA in uplink for high data rate script when consider the targeted performance metrics on multi user variety gain. Hence, they predict that OFDMA is used in downlink and SC-FDMA is used in uplink [3].

Considering the UMTS-LTE technology in downlink in the system bandwidth and SNR efficiency, there is a study about the increasing of MIMO capacity conducted by Pedro Vierra, Paula Queluz and Antonio Rodrigues [4]. They investigated in this study, "the system bandwidth efficiency for LTE framework is initially calculated. Secondly, SNR efficiency is approximated using curve fitting via Adaptive Modulation and Coding (AMC). The use of fitting function is an attenuated and truncated form of the Shannon bound in order to approximate the LTE combined spectral efficiency for the Modulation and Coding Set (MCS). Hence, the total capacity estimated results are calculated through different multi antenna configurations since MIMO exposes large capacity gains compared to SISO."

In Multiple Input Multiple Output (MIMO) systems, the antenna array configuration at the Mobile Station (MS) and Base Station (BS) has a significant role in the existing channel capacity at sample location as emphasized by Pedro Vierra, Paula Queluz and Antonio Rodrigues. After the number of antennas and distance between antennas are changed, MIMO configuration has been shown to be optimized [4].

The analysis of the LTE theoretical downlink and uplink peak rates are presented by Dongzhe Cui. In addition, he provides practical peak rates in the ideal RF condition in Lab. [5]

The propagation path loss models for cellular communication are analyzed in detail by Aktül Kavas. In this study, these models are analyzed and calculated for different environment parameters, different frequencies, different distances and different base station transmitter heights. Besides, mobile radio system design parameters are presented in order to determine cell radius, receiver signal power and data capacity along with these calculations [6].

1.2.Objectives

This thesis examines that information is offered about different methods for capacity and coverage area calculations. This study also tested whether Shannon Capacity Equality or using software (like ATOLL) tools are preferred by today operators on sample.

1.3.Organization of the Thesis

Nowadays, the demand towards mobile phones that require high data rates with the advancement of technology in real time games, television, internet and video streaming applications has rapidly increased. In mobile networks, long-term evolution (LTE) standard was improved by the Third Generation Partnership Project (3GPP) to meet the increasing demand. Today, on February 28th, 2017[1], 790 operators have commercially launched LTE in 201 countries, according to data released this week by GSA (Global mobile Suppliers Association) in its latest update of the Evolution to LTE report.

In chapter 2, the evolution of mobile communication systems is analyzed

In chapter 3, the properties of LTE are examined. After that, frame structure and modulations of access technologies of LTE standard are used for description.

In chapter 4, the modules required to calculate the capacity of LTE radio interface is explained and the capacity of radio interface is calculated.

In chapter 5, the modules required to calculate the coverage of LTE radio interface is explained and the capacity calculations for sample values is calculated.

In chapter 6, the planning and optimization of a sample test network were conducted. The question whether Shannon Capacity Equality or software (like ATOLL) tools are used by today operators is answered.

2. INTRODUCTION to MOBILE COMMUNICATION

2.1. Evolution of Cellular Networks

We have seen the enormous development in cellular mobile networks within just last 10 years. These networks are First Generation (1G), Second Generation (2G), Third Generation (3G) and Fourth Generation Systems (4G). Firstly, we used 1G which has been replaced by 2G and 3G networks. Today, on the other hand, 4G systems are being developed. In this chapter, the evolution of cellular networks such as 1G, 2G, 2.5G, 2.75G, 3G and 4G systems [7] is analyzed.
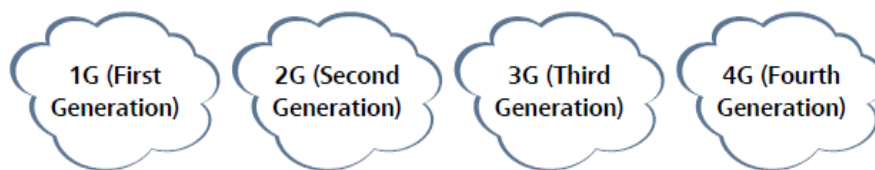
Figure 1 Evolution of Cellular Networks [7]
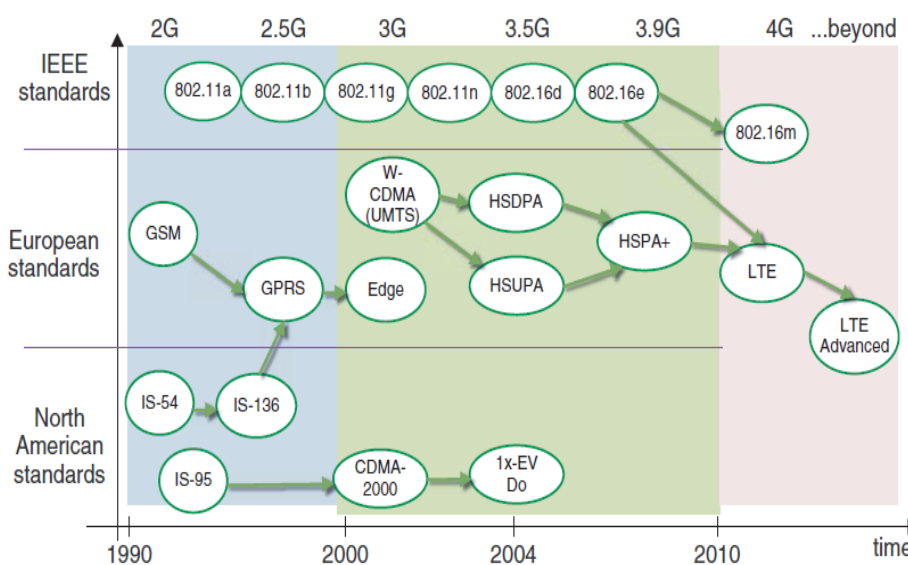
Figure 2 Evolution of wireless standards[8]

4

Technology	Theoretical peak data rate(at low mobility)
GSM	9.6 kbps
IS-95	14.4 kbps
GPRS	171.2 kbps
EDGE	473 kbps
CDMA-2000 (1xRTT)	307 kbps
WCDMA(UMTS)	1.92 Mbps
HSDPA(Rel 5)	14 Mbps
CDMA-2000(1x EV-DO)	3.1 Mbps
HSPA+(Rel 6)	84 Mbps
WIMAX(802.16e)	26 Mbps
LTE(Rel 8)	300 Mbps
WIMAX(802.16m)	303 Mbps
LTE-Advanced(Rel 10)	1 Gbps

Table 1 Peak data rates of various wireless standards introduced over the last two decades [8]

2.1.1. First Generation Mobile Systems

Since the beginning of 1G in mobile communication around 1980s, significant changes have been experienced and this technology reached approximately 20 million subscribers with the rate of approximately 35-50 %. The 1G mobile system was based on analogue modulation techniques [2].

All personal based Frequency Modulation (FM) systems were conducted by these analogue systems. Thus, security, any essential data service and international roaming capability were enough with this technology.

2.1.2. Second Generation Mobile Systems

The approach of Second Generation (2G) started in late 1980s. The 2G systems applied digital multiple access technology such as TDMA and CDMA [2].

✓ **Global System for Mobile communications (GSM):** The most successful version of all 2G technologies is GSM. European Telecommunications Standards Institute (ETSI) for Europe initially improved it and designed to achieve in the 900MHz and 1800MHz frequency bands. It has widely ensured world support today and is available for deployment on many other frequency bands, such as 850MHz and 1900MHz. Being described as tri-band or quad-

band, it offers support for various frequency bands on a single device. GSM is TDMA which employs 8 timeslots on a 200 kHz radio carrier.

The abovementioned 2G digital systems offer advanced services such as Short Message Service (SMS) and circuit switched data as well as being digital systems and offering improved capacity and security properties.

2.1.3. 2.5G Systems

Most 2G systems have been improved. For instance, GSM was expanded by means of General Packet Radio System (GPRS) for the purpose of offering a support to efficient packet data services, and raising data rates.

GRPS is regularly referred to as 2.5G while this feature does not fulfill 3G requirements. A comparison between 2G and 2.5G systems is clarified in Table 2[7].

2.1.4. 2.75G Systems

GSM/GPRS systems are added to Enhanced Data Rates for Global Evolution (EDGE) which almost quadrupled the throughput of GPRS w. The theoretical data rate of 473.6k bit/s helps service providers offer effective multimedia services. EDGE is usually classified as 2.75G just as GPRS since they do not involve all features of a 3G system.

System	Service	Theoretical Data Rate	Typical Data Rate
2G GSM	Circuit Switched Data	9.6kbit/s or 14.4kbit/s	9.6kbit/s or 14.4kbit/s
2.5G GPRS	Packet Switched Data	171.2kbit/s	4kbit/s to 50kbit/s
2.75G EDGE	Packet Switched Data	473.6kbit/s	120kbit/s

Table 2 2.5G and 2.75G GSM/GPRS Systems [7]

2.1.5. Third Generation Mobile Systems

In the world of mobile technology, many more industries in telecommunication have experienced a revolutionary change by 3G. In addition to improving the speed of communication, the aim of this technology is to supply several value added services. Since the necessary bandwidth is obtained by the 3G spectrum, these services are available [2]. IMT-2000 standard defines that a 3G technology should provide higher transmission rates.

2.1.6. Fourth Generation Mobile Systems

LTE technology is referred to as 3.9G or Super 3G. LTE will be capable of reaching 150 Mbps download rates for multi-antenna (2x2), MIMO for the highest category terminals during the use of OFDMA. As for the terminals, upload rates will ensure the efficient data transfer in 50 Mbps range [2].

Table 3 presents the summary of the main performance necessaries of the first release of LTE. A good number of figures are also presented regarding the performance of the most recent version of UMTS, – HSDPA/HSUPA Release 6 – at the time when the LTE requirements, here referred to as the reference baseline, were determined [9].

		Absolute requirement	Comparison to Release 6	Comment
Downlink	Peak transmission rate	>100 Mbps	7 x 14,4 Mbps	LTE in 20 MHz FDD, 2x 2 spatial multiplexing.
	Peak spectral efficiency	>5 bps/ Hz	3 bps/Hz	Reference: HSDPA in 5 MHz FDD, single antenna transmission
	Average cell spectral efficiency	>1.6-2.1 bps/Hz/cell	3-4 x 0.53 bps/Hz/ cell	LTE: 2x2 spatial multiplexing, Interference Rejection Combining (IRC) receiver. Reference: HSDPA, Rake receiver, 2 receive antennas
	Cell edge spectral efficiency	>0.04-0.06 bps/Hz/user	2-3 x 0.02 bps/Hz	As above, 10 users assumed per cell
	Broadcast spectral efficiency	>1 bps /Hz	N/A	Dedicated carrier for broadcast mode
Uplink	Peak transmission rate	>50 Mbps	5 x 11 Mbps	LTE in 20 MHz FDD, single antenna transmission.
	Peak spectral efficiency	>2.5 bps /Hz	2 bps /Hz	Reference: HSUPA in 5 MHz FDD, single antenna transmission
	Average cell spectral efficiency	>0.66-1.0 bps/Hz/cell	2-3 x 0.33 bps/Hz	LTE: single antenna transmission, IRC receiver. Reference: HSUPA, Rake receiver, 2 receive antennas
	Cell edge spectral efficiency	>0.02-0.03 bps/Hz/user	2-3 x 0.01 bps/Hz	As above, 10 users assumed per cell
System	User plane latency(two way radio delay)	<10 ms	One fifth	
	Connection set-up latency	<100 ms		Idle state → active state
	Operating bandwidth	1.4- 20 MHz	5 MHz	(initial requirement started at 1.25 MHz)
	VoIP capacity	NGMN preferred target expressed in [2] is > 60 sessions/ MHz/ cell		

Table 3 Abstract of the performance necessary goals for LTE [9]

CHAPTER 3

3. INTRODUCTION to LTE

3.1. Wireless Spectrum

Figure 3 presents the LTE frequency bands for paired bands in 3GPP specifications and Figure 4 presents those for unpaired bands. There are 17 paired bands and 8 unpaired bands available right now and more bands will be involved during the standardization process. Some of the bands are currently used by other technologies and LTE can coexist with the legacy technologies.

Operating band	3GPP name	Total spectrum	Uplink [MHz]	Downlink [MHz]
Band 1	2100	2x60 MHz	1920-1980	2110-2170
Band 2	1900	2x60 MHz	1850-1910	1930-1990
Band 3	1800	2x75 MHz	1710-1785	1805-1880
Band 4	1700/2100	2x45 MHz	1710-1755	2110-2155
Band 5	850	2x25 MHz	824-849	869-894
Band 6	800	2x10 MHz	830-840	875-885
Band 7	2600	2x70 MHz	2500-2570	2620-2690
Band 8	900	2x35 MHz	880-915	925-960
Band 9	1700	2x35 MHz	1750-1785	1845-1880
Band 10	1700/2100	2x60 MHz	1710-1770	2110-2170
Band 11	1500	2x25 MHz	1427.9-1452.9	1475.9-1500.9
Band 12	US700	2x18 MHz	698-716	728-746
Band 13	US700	2x10 MHz	777-787	746-756
Band 14	US700	2x10 MHz	788-798	758-768
Band 17	US700	2x10 MHz	704-716	734-746
Band 18	Japan800	2x30 MHz	815-830	860-875
Band 19	Japan800	2x30 MHz	830-845	875-890

Figure 3 Frequency bands for paired bands in 3GPP specifications [10]

Operating band	3GPP name	Total spectrum	Uplink and downlink [MHz]
Band 33	UMTS TDD1	1x20 MHz	1900-1920
Band 34	UMTS TDD2	1x15 MHz	2010-2025
Band 35	US1900 UL	1x60 MHz	1850-1910
Band 36	US1900 DL	1x60 MHz	1930-1990
Band 37	US1900	1x20 MHz	1910-1930
Band 38	2600	1x50 MHz	2570-2620
Band 39	UMTS TDD	1x40 MHz	1880-1920
Band 40	2300	1x50 MHz	2300-2400

Figure 4 Frequency bands for unpaired bands in 3GPP specifications [10]

User equipment category	Maximum L1 data rate downlink	Maximum number of DL MIMO layers	Maximum L1 data rate uplink	3GPP release
Category 1	10.3 Mbit/s	1	5.2 Mbit/s	Release 8
Category 2	51.0 Mbit/s	2	25.5 Mbit/s	Release 8
Category 3	102.0 Mbit/s	2	51.0 Mbit/s	Release 8
Category 4	150.8 Mbit/s	2	51.0 Mbit/s	Release 8
Category 5	299.6 Mbit/s	4	75.4 Mbit/s	Release 8
Category 6	301.5 Mbit/s	2 or 4	51.0 Mbit/s	Release 10
Category 7	301.5 Mbit/s	2 or 4	102.0 Mbit/s	Release 10
Category 8	2,998.6 Mbit/s	8	1,497.8 Mbit/s	Release 10
Category 9	452.2 Mbit/s	2 or 4	51.0 Mbit/s	Release 11
Category 10	452.2 Mbit/s	2 or 4	102.0 Mbit/s	Release 11

Table 4 Uplink and Downlink Speeds according to terminal categories [11]

E-UTRA is the air interface standard of LTE of 3GPP. This standard provides peak download rates of 299.6 Mbit/s for 4x4 antennas, and 150.8 Mbit/s for 2x2 antennas with 20 MHz of spectrum. The LTE Advanced supports up to 8x8 MIMO antenna configurations with peak download rates of 2,998.6 Mbit/s in an aggregated 100 MHz channel [11].

3.2. AMC

The criteria for determining the quality of the signal received by a UE in cellular communication systems can be defined as the channel quality from the serving cell, the noise level, and the level of interference from other cells. The transmitter is expected to match the information data rate for each user to the variations in the received signal so that system capacity and coverage for a given transmission power can be optimized [9]. It is usually referred to as link adaptation based on AMC. The AMC comprises the modulation Scheme and code rate.

- ✓ **Modulation Scheme:** Low-order modulation (such as QPSK) is stronger and also can tolerate higher levels of interference despite offering a lower transmission bit rate. However, high-order modulation (such as 64 QAM), offers a higher bit rate, yet it is more prone to errors due to its higher sensitivity to interference, noise and channel estimation errors. In this sense, high-order modulation can be useful only when the Signal to Interference and Noise Ratio (SINR) are high enough.

- ✓ **Code rate:** For any modulation, the code rate can be preferred depending the radio link: a lower code rate can be selected in low channel conditions and a higher code rate can be preferred in case of high SINR.

The eNodeB ordinarily chooses the Modulation and Coding Scheme (MCS) on the basis of the Channel Quality Indicator (CQI) feedback transmitted by the UE in the uplink for the downlink data transmissions in LTE.

For the LTE uplink transmissions, the link adaptation process is in parallel with the downlink including the selection of MCS which is also controlled by the eNodeB. However, the eNodeB can straightly estimate the supportable uplink data rate via channel sounding.

The list of modulation code rates and schemes with CQI values supported by 3GPP LTE standards is presented in Table 5.

CQI Index	Modulation	Code Rate	Efficiency
0	Out of range		
1	QPSK	78	0.1523
2	QPSK	120	0.2344
3	QPSK	193	0.3770
4	QPSK	308	0.6016
5	QPSK	449	0.8770
6	QPSK	602	1.1758
7	16QAM	378	1.4766
8	16QAM	490	1.9141
9	16QAM	616	2.4063
10	64QAM	466	2.7305
11	64QAM	567	3.3223
12	64QAM	666	3.9023
13	64QAM	772	4.5234
14	64QAM	873	5.1152
15	64QAM	948	5.5547

Table 5 4-bit CQI table for modulation schemes [15]

3.3.OFDMA and SC-FDMA

OFDMA is preferred for the downlink and SC-FDMA for the uplink by LTE. OFDMA is unanimously considered as the most appropriate technique for the downlink in order to achieve high spectral efficiency [3]. On the other hand, the LTE of 3GPP employs SC-FDMA for the uplink due to its low PAPR properties compared to OFDMA.

OFDMA, as a multiple access scheme, is built upon the OFDM modulation technique. The OFDM signal can be produced through the IFFT. In an OFDM system, the available spectrum is subdivided into multiple and mutual orthogonal subcarriers. A low rate data stream is used for the independent modulation of each of these subcarriers which can carry independent information streams. Figure 5 presents how the OFDM technique is carried out for a signal with 5 MHz bandwidth.
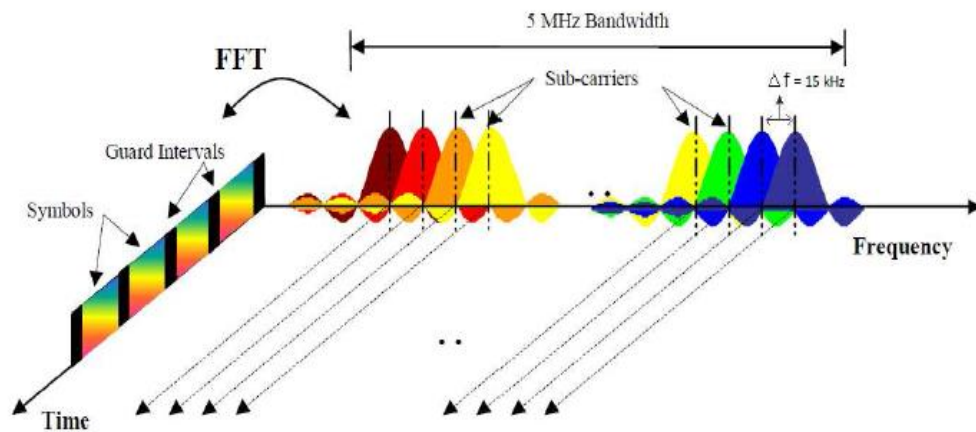
Figure 5 Frequency and time displaying of an OFDM Signal [12]

In the frequency domain, the 5 MHz bandwidth is divided into a high number of orthogonal subcarriers which are closely spaced. The constant spacing included in the subcarriers in LTE is $\Delta f = 15$ kHz. The downlink modulation schemes can differ between QPSK, 16QAM and 64QAM in E-UTRA. In the time domain, a guard interval is added to each symbol with the purpose of combating inter-OFDM-symbol interference (ISI) because of the channel delay spread. The guard interval is a cyclic prefix (CP) inserted prior to each OFDM symbol in E-UTRA. A sub-channel refers to a group of subcarriers. Figure 6 illustrates the multiple accesses in OFDMA as achieved by logically allocating different sub-channels to various users on demand basis [12].
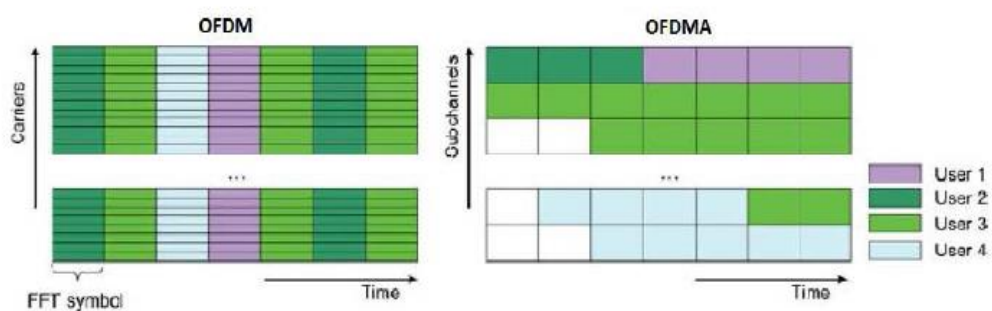
Figure 6 Variance among channel allocation using OFDM and OFDMA [13]

OFDMA meets the LTE requirement for the spectrum flexibility and enables cost-efficient solutions for very wide carriers by means of high peak rates. OFDM has a variety of pros to be summarized as follows:

    ✓ Providing robustness to multipath fading.

13

✓ Yielding a highly spectral efficient system as these subcarriers is mutually orthogonal; overlapping between them is permitted [3].

Although OFDMA is deemed as the optimum solution for the downlink, it is still less suitable for the uplink due to its weaker PAPR properties which finally cause a poor uplink coverage. Because of this reason, the SC-FDMA is preferred as a solution for the uplink. A SC-FDMA signal can be generated via DFT spread OFDM digital signal processing. The main functioning principle of it is the same as OFDM; hence, the same advantages of multipath mitigation and low-complexity equalization can be obtained [3]. The dissimilarity is regarding the fact that the data symbols spread all over the subcarriers transmitting information and create a virtual single-carrier structure in a SC-FDMA signal.
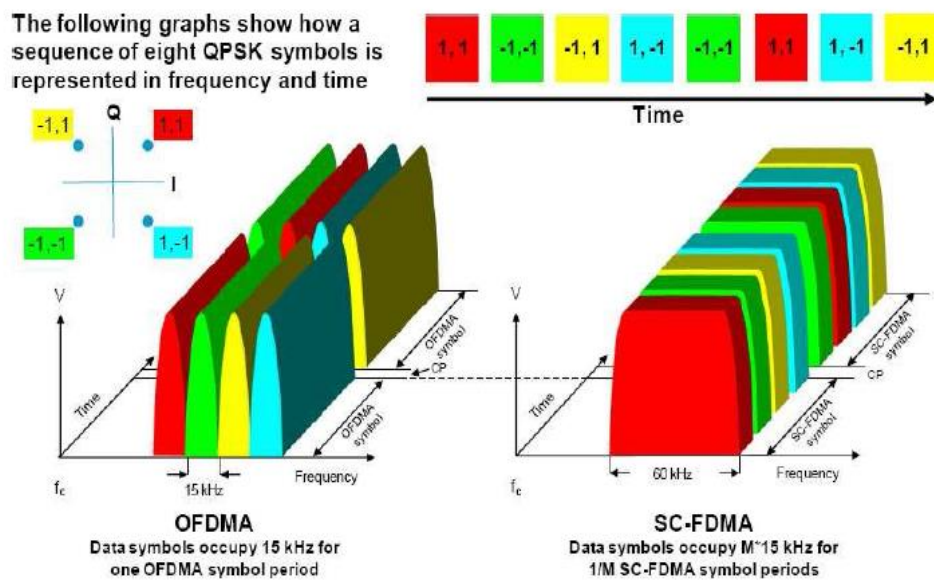
Figure 7 Transmitting OFDMA and SC-FDMA a sequence of QPSK data symbols [14]

Figure 7 presents the exemplified usages of four (M) subcarriers over two symbol periods by QPSK modulation. The most apparent difference between the two schemes is that OFDMA transmits four QPSK data symbols in parallel, one per subcarrier, while SC-FDMA transmits four QPSK data symbols in a series at four times with each data symbol with Mx15 kHz bandwidth. As presented, the OFDMA signal seems to be multi-carrier and the SC-FDMA signal is more like a single-

14

carrier [14]. It should also be noted that OFDMA and SC-FDMA symbol lengths are the same, at 66.7 µs.

SC-FDMA presents a lower PAPR compared to OFDM. This particular feature makes SC-FDMA appealing for uplink transmissions, since the transmitted power efficiency is useful for the user equipment (UE) and all symbols are available in all subcarriers [3].

3.4. LTE Physical Layer

In this section, some more details of OFDMA, SC-FDMA and frame structures are described at physical layer level. The concepts and parameters will further be used in Section 4.

3.4.1. OFDMA

In accordance with the OFDMA principle, each of the center frequencies is selected for the sub-carriers from a set which has differentiations in the frequency domain where the neighboring sub-carriers have zero value at the sampling for the given sub-carrier, as demonstrated in Figure 8[10].
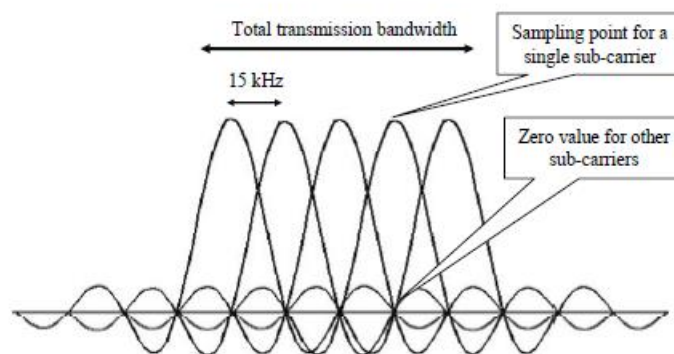
Figure 8 Maintaining the sub-carriers' orthogonality [10]

3.4.2. OFDMA and SC-FDMA Resource Structure

OFDM uses a high number of narrow sub-carriers in order to achieve multi-carrier transmission. The physical resource for the basic LTE downlink can be seen as a time-frequency grid, as presented in Figure 9.
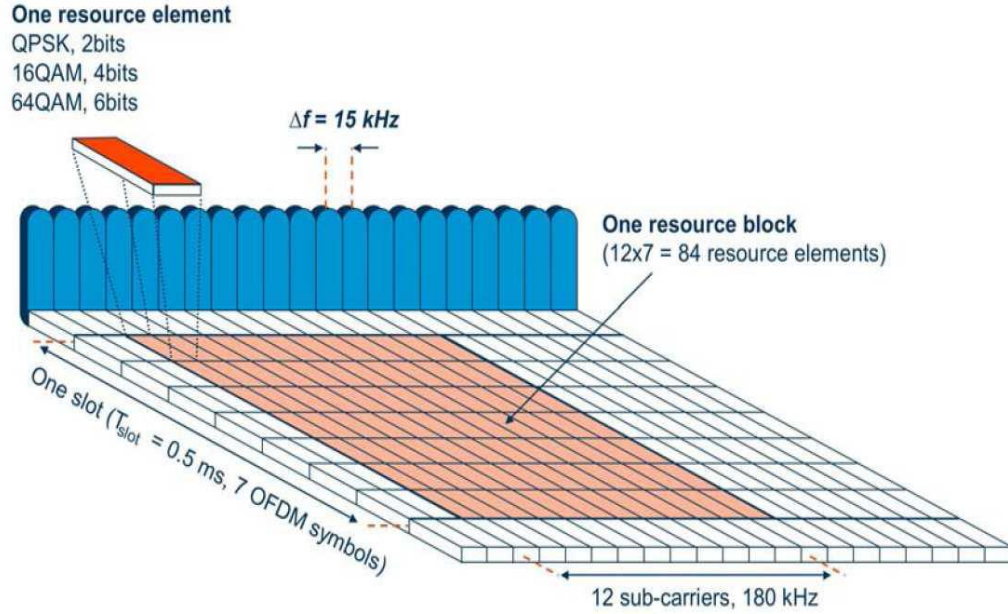
Figure 9 LTE downlink physical resource grid based on OFDM [16]

A CP is appointed as guard time for each OFDM symbol. Furthermore, the OFDM symbol duration time is $1/\Delta f$ + cyclic prefix (CP).

All of the OFDM symbols are grouped within resource blocks. A resource block refers to the smallest unit of bandwidth assigned by the base station scheduler. Total size of the resource blocks is 180 kHz involving 12 subcarriers in the frequency domain and 0.5 ms with 7 OFDM symbols (with the normal CP) in the time domain. There are two slots in each 1 ms Transmission Time Interval (TTI). Many resource blocks are allocated for each user in the time–frequency grid. The bit-rate increases in parallel with the number of the blocks a user owns and the number of the preferred modulation used the resource elements. The resource block size does not vary by bandwidth. The list in Table 6 demonstrates the number of resource blocks for various LTE bandwidths.

Channel bandwidth [MHz]	1.4	3	5	10	15	20
Number of resource blocks	6	15	25	50	75	100

Table 6 The number of the resource blocks for various LTE bandwidths [17]

There are 6 or 7 OFDM symbols in a downlink slot based on whether the configured cyclic prefix is extended or normal. The extended cyclic prefix can cover

larger cell sizes with higher delay spread of the radio channel. Table 7 demonstrates the cyclic prefix lengths.

Configuration	Resource block size N_{SC}^{RB}	Number of symbols N_{symb}^{DL}	Cyclic Prefix length in samples	Cyclic Prefix length in μs
Normal cyclic prefix $\Delta f = 15$ kHz	12	7	160 for first symbol 144 for other symbols	5.2 μs for first symbol 4.7 μs for other symbols
Ext. Cyclic prefix $\Delta f = 15$ kHz	12	6	512	16.7 μs

Table 7 Downlink frame structure parameterization [18]

As demonstrated in Figure 10, the LTE uplink SC-FDMA has an alike structure with the downlink resource grid. The uplink is also presented in Table 6 and Table 7.

As demonstrated in Figure 11, UE are always assigned to contiguous resources in the LTE uplink, which is different from the downlink.

1 subframe = 1 ms = 14 SC-FDMA symbols
(normal cyclic prefix)

1 slot = 0.5 ms = 7 SC-FDMA symbols
(normal cyclic prefix)

Resource Block
(12 subcarriers in frequency
domain, 1 slot in time domain)

Resource Element
(k, l)

Subcarriers (numbered with index k)

k = 0

l = 0

SC-FDMA symbols (numbered with index l)
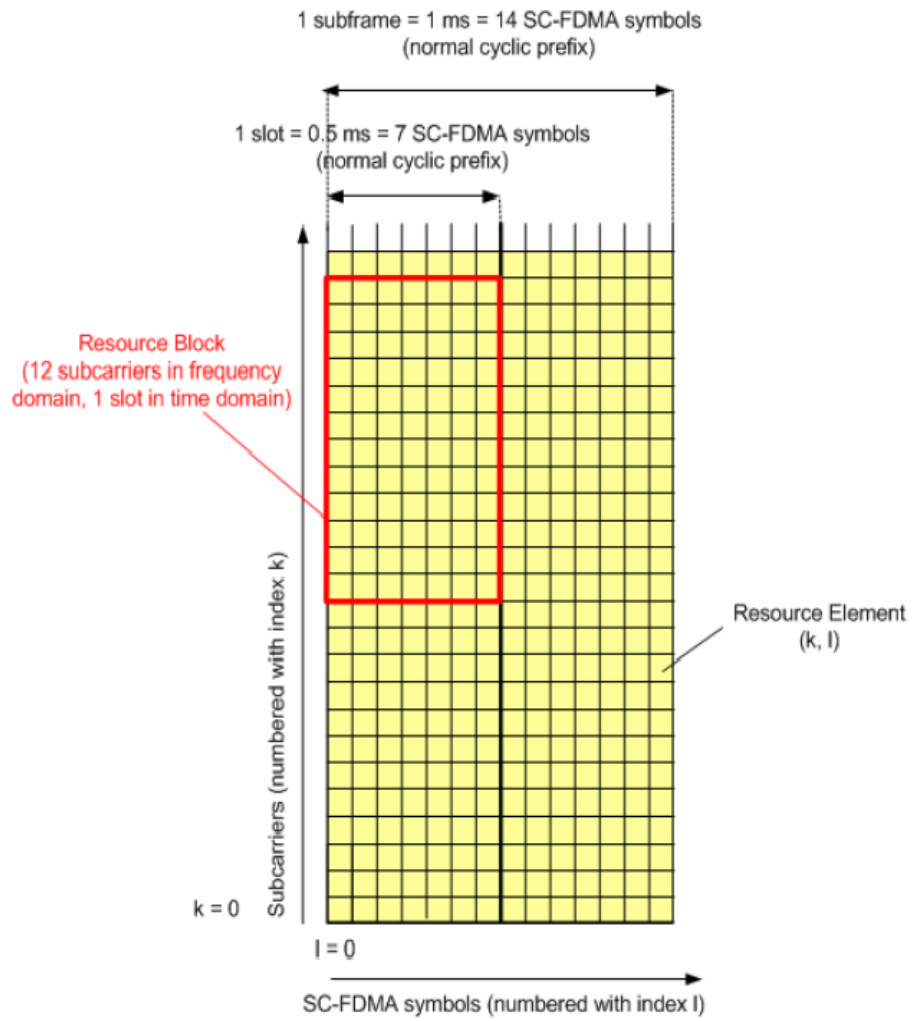
Figure 10 Uplink SC-FDMA resource grid [18]

≈200 kHz

0.5 ms

User A
User B
User C
User D

Time

Frequency

Downlink

Time
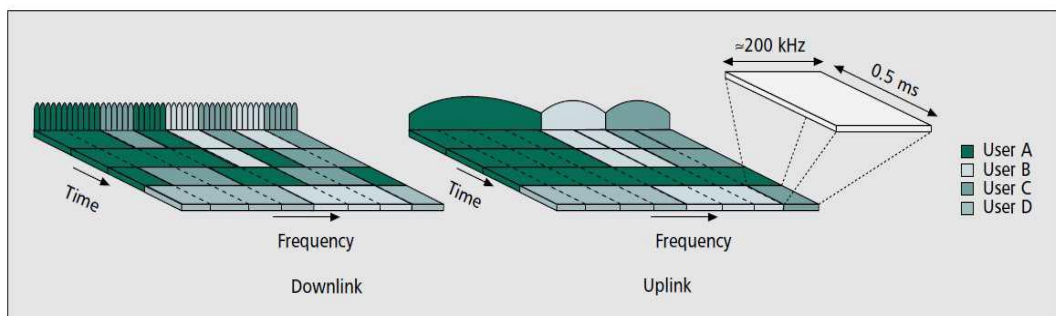
Frequency

Uplink

Figure 11 Time-frequency structure for downlink and uplink [19]

18

3.4.3. Reference Signal

The transmitters and receivers are expected to estimate the channel with the purpose of conducting a coherent demodulation of various physical channels at both the downlink and the uplink. One of the basic techniques of the channel estimation in LTE is to enter the known reference symbols into the OFDM/SC-FDM time frequency grid.

Figure 12 illustrates an example of reference symbols for 1 antenna transmission in the downlink direction. The reference signals structures vary by different antenna configurations, which are further discussed in Section 4.3.3. Three kinds of reference signals can be defined for the LTE downlink [20] being, cell-specific downlink reference signals, UE-specific reference signals and MBSFN reference signals. Only the first one, Cell specific downlink reference signals, is taken into consideration in this thesis, since it is transmitted in each downlink sub-frame and spans the entire downlink cell bandwidth so that it has a vital impact on the efficiency of channel bandwidth.
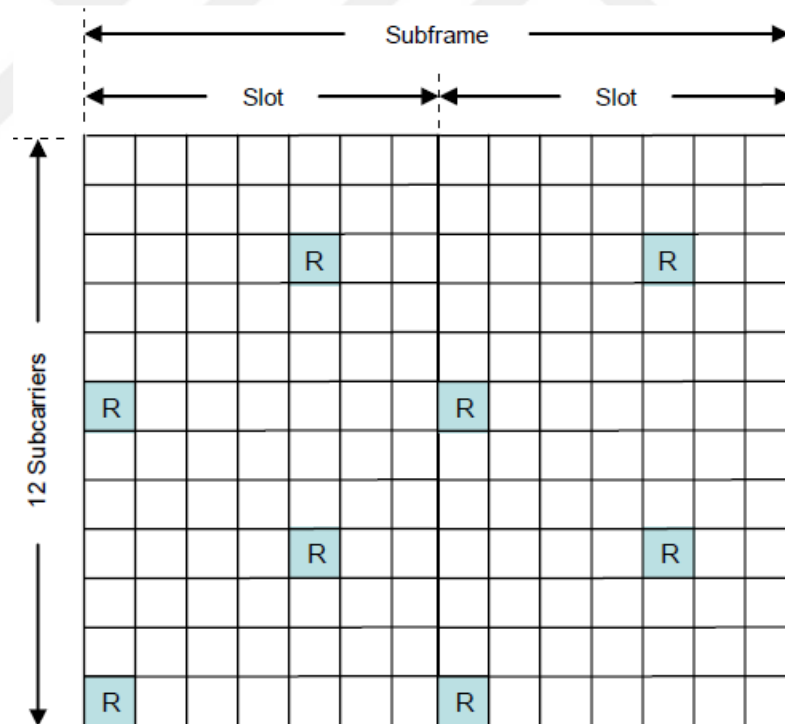
Figure 12 LTE downlink reference signals (normal cyclic prefix) [9]

In the uplink direction, the principle for the uplink reference-signal transmission is different compared to the downlink because of the importance attached to low power variations in the uplink transmissions. There are two types of

reference signals defined for the LTE uplink, being the demodulation reference signal (DRS) and sounding reference signal (SRS) [20]. The uplink reference signal mentioned in this thesis refers to the uplink DRS for the convenient use of the term. As demonstrated in Figure 13, a reference signal is transmitted within the fourth symbol of each uplink slot during the Physical Uplink Shared Channel (PUSCH) transmission. Therefore, there are two reference-signal transmissions; being one in each slot within each sub-frame.
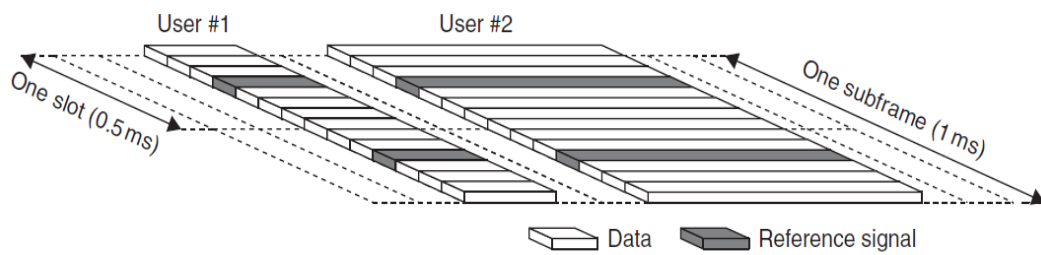
Figure 13 Transmission of uplink reference signals in case of PUSCH transmission [20]

3.5. Synchronization

A UE asking to access to a LTE cell must first initiate a cell search procedure. This procedure involves a series of synchronization stages by which the UE detects the required time and frequency parameters for the demodulation of the downlink and transmission of the uplink signals with accurate timing; furthermore, the UE obtains some crucial system parameters [9]. The synchronization signal is defined to be the downlink physical signal which corresponds to a set of resource elements which is used by the physical layer, however it does not transmit any information originated from higher layers [18].

The synchronization procedure uses two particularly designed physical signals broadcasted in each cell, being the Primary Synchronization Signal (PSS) and the Secondary Synchronization Signal (SSS). The latter carries the physical layer cell identity group while the former one carries the physical layer identity. Both time and frequency synchronization can be possible through the detection of these two signals. [9].

3.6. System Information Broadcast

Following the procedures of the cell search and synchronization, the terminal must obtain information regarding the cell system. This information is broadcasted by the network to the terminals again and again. In classical cellular systems, the basic system information, which ensures the configuration and operation of other channels in the cell, is transmitted by a BCH. The broadcast system information can be categorized under two titles:

- ✓ The MIB comprises a limited number of the most frequently transmitted parameters being fundamental for beginning access to the cell. It is carried on the PBCH.
- ✓ The other SIBs are multiplexed together with the unicast data is transmitted on the Physical Downlink Shared Channel on the physical layer [9].

This procedure is applied for the downlink direction and this thesis is solely confined to the PBCH used in particular for the later calculation.

3.7. Random Access Procedure

An essential inquiry for any cellular system is to enable the terminal to request a connection setup, which is often referred to as random access. The random access procedure is preferred with the purpose of requesting an initial access, as a part of handover, or re-establishing the uplink synchronization.

The LTE random access procedure can take place in two forms enabling access to be either contention-based or contention-free.

- ✓ Contention-based: In this procedure, the UE randomly chooses a random access preamble signature. Accordingly, multiple UEs can simultaneously transmit the same signature. This procedure is applied in all the cases which include the random access.
- ✓ Contention-free: In this procedure, the base station in LTE (eNodeB) can alternatively prevent the ongoing contention by allocating a dedicated signature to a UE. This procedure is more rapid than the contention-based access a factor that is especially significant for the case of the time-critical handover [9].

21

While the Contention-free is applied in more limited number of scenarios like a handover, the Contention-based procedure is applied in all cases including the random access. This thesis takes solely the random access procedure into consideration.
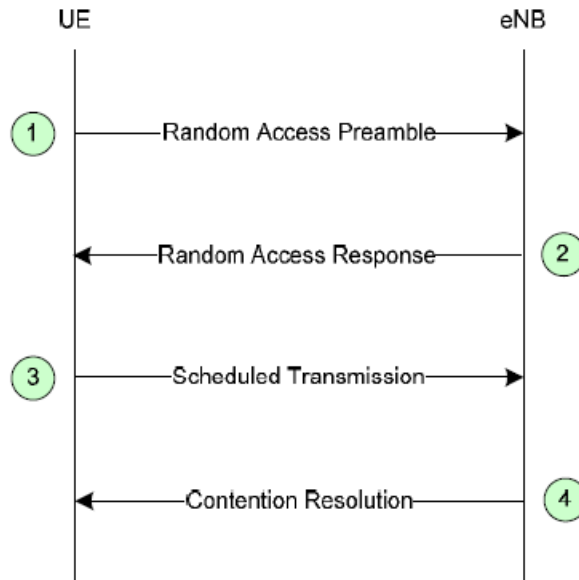
Figure 14 Contention based Random access procedure [21][9]

The first step of the procedure, as presented in Figure 14, is the transmission of a random access preamble whose aim is to indicate the presence of a random-access attempt to the base station and to enable the base station to estimate the delay between the eNodeB and the terminal. Only the first step is taken into consideration in this thesis, since it involves the preamble overheads to the uplink transmission. This particular step is further discussed in the Section 4.3.6.

3.8.MIMO technology

MIMO systems form a remarkable part of LTE and meet the hopeful necessaries for throughput and spectral efficiency [21]. MIMO can be defined by the use of multiple antennas at the sides of both the transmitter and receiver. The baseline configuration is set as a 2x2 configuration for MIMO for the LTE downlink. For instance, two transmit antennas are placed at the base station and two receive antennas at the terminal side.

MIMO has two different functionality modes. Different advantages are offered by the use of either MIMO mode. The Spatial Multiplexing ensures the transmission of different streams of data simultaneously on the same resource

block(s) by exploiting the spatial dimension of the related radio channel, so that, the data rate or capacity can be advanced [21]. The Transmit Diversity mode is another mode that can be preferred to exploit diversity and enhance the strength of data transmission. This thesis is confined only to the spatial multiplexing mode at the moment of the calculation of the LTE capacity and data rate.

As illustrated in Figure 15, it is possible to exemplify a 4 x 4 antenna configuration (4 transmit antenna and 4 receiver antenna) in which each receiver antenna may receive the data streams from all of the transmit antennas. The Transmission Channel Matrix H, as presented below, can be used to illustrate the transmission relationship. Of all the coefficients, h_{ij} refers to the transmit antenna; j to the receive antenna; i to all possible paths between transmitter and receiver sides.
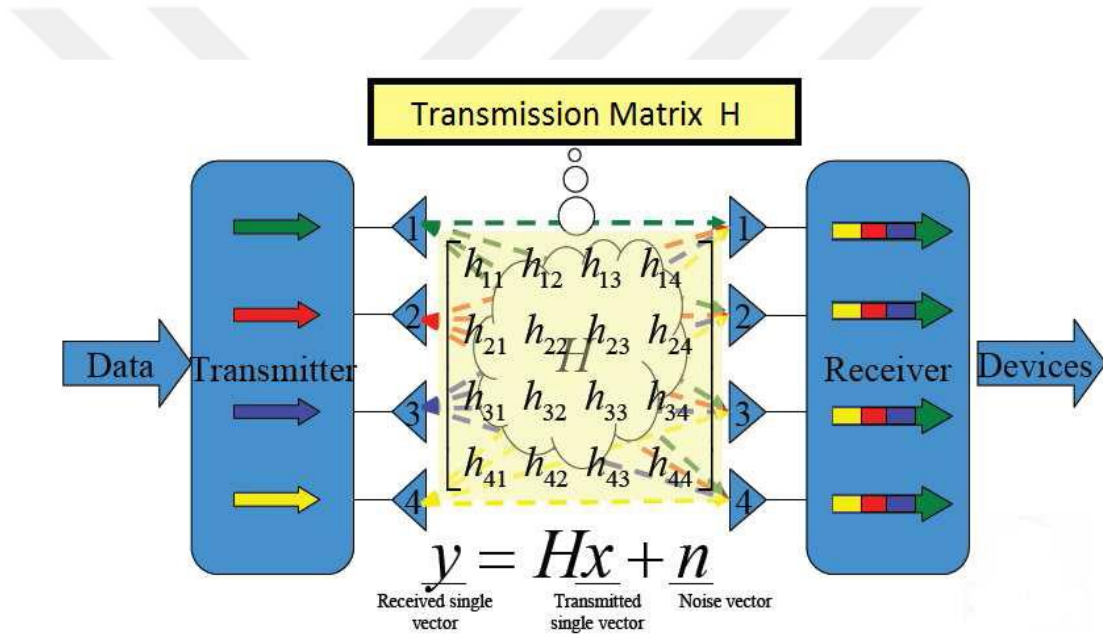
Figure 15 MIMO Transmission [22]

Where the receive vector is y, the transmit vector is x, the noise vector is n and the transmission channel matrix is H, the MIMO transmission can be described with the following formula:

$$y = Hx + n \tag{3.1}$$

In an M x N antenna configuration, the minimum value of M and N is given to the number of data streams which can be transmitted in parallel over the MIMO channel, is given by and this number limited by the rank of the transmission matrix H. For example, a 4 x 4 MIMO system can be preferred to transmit four or less data streams.

In the spatial multiplexing mode, the transmitted data streams can belong either to a single user MIMO/SU-MIMO or various multi user MIMO/MU-MIMO (see Figure 16).
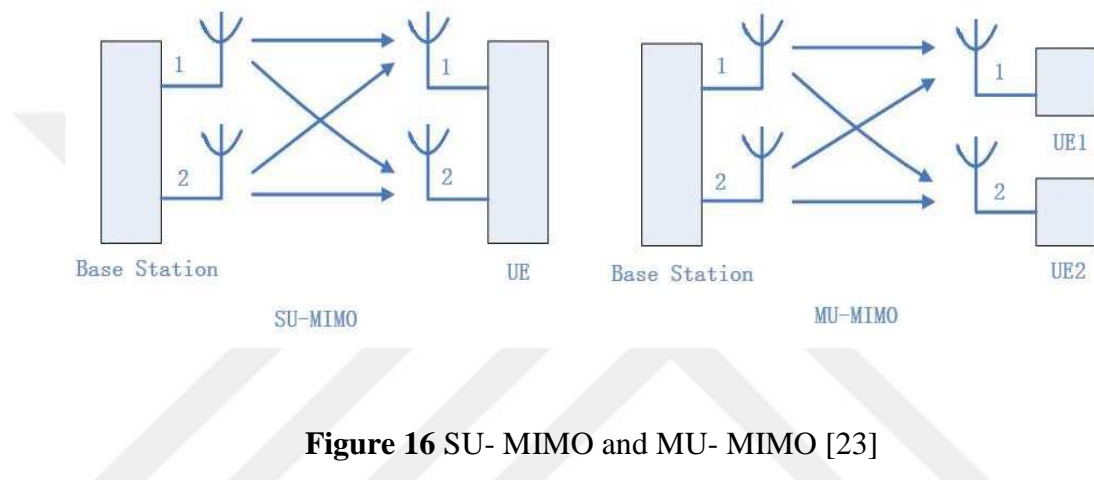
Figure 16 SU- MIMO and MU- MIMO [23]

While SU- MIMO raises the data rate of only one user, MU- MIMO raises the overall capacity.

CHAPTER 4

4. CAPACITY PLANNING in LTE

While the LTE channel is being modeled, transmission over the AWGN channel with a two-sided noise power spectral density $N_0/2$ with perfect CSI is accepted.

A channel bandwidth may be split into Q flat-fading sub-channels $\mathbf{H}(f_q)$, f_q the qth sub-carrier central frequency, and referred to resource block with a frequency separation of 180 kHz in the LTE system. The smallest unit of bandwidth allocated by the base station programmer gives name to the resource block.

In consideration of the channel eigen-analysis [4], the channel matrix $\mathbf{H}$ (f_q) can offer K_q parallel sub-channels with a variety of power gains (eigenvalues), $\alpha_{k,q}$, where,

$$K_q = Rank\left(R(f_q)\right) \le Min(U,V) \tag{4.1}$$

The functions *Rank* () and *Min* () return the matrix rank and the minimum value of the arguments. *U* refers to the number of Base Station (BS), and *V* to the Mobile Station (MS) antenna. This corresponds to the concept of the MIMO spatial multiplexing. [24].

In case that the channel is known at both Transmitter (T_x) and Receiver (R_x) and is used to compute the antennas optimum weight, the power gain in the $(k,q)^{th}$ eigenmode channel is detected by the $\alpha_{k,q}$ eigenvalue, i.e., the SNR for the $(k,q)^{th}$ sub-channel, $v_{k,q}$, is equal to,

$$v_{k,q} = \alpha_{k,q}\beta_{k,q}\frac{S}{N} \tag{4.2}$$

The type of power assigned to the $(k,q)^{th}$ sub-channel is named the $\beta_{k,q}$. The *S/N* refers to the radio link SNR. The $\beta_{k,q}$ value is defined as the sub-channel power

allocation scheme. We assume the Uniform Power Allocation [4] across all sub-channels to be

$$\beta_{k,q} = \frac{P_{TX}}{RQ}$$

(4.3)

Where; P_{TX} is the total transmitted power, R is the resource block number per sub-channel and Q is the number of the sub-channels. Here, R = 1 and Q can be found from Table 6 for the given channel bandwidth.

The noise power σ_N^2 is calculated as [25]

$$\sigma_N^2 = kT + 10\log_{10}(B_w) + NF$$

(4.4)

Where; kT is the thermal noise density, defined to be -174 dBm/Hz where k is Boltzmann's constant (1.380662 x 10^{-23}) and in LTE specifications, and T is the temperature of the receiver (assumed to be 15°C). B_w is the channel bandwidth in Hz. NF is the noise figure which is defined to be 5 for the eNodeB in LTE [9].

4.1. Shannon Capacity Equality

According to Shannon–Hartley theory, the Shannon capacity bound formula, as indicated in expression 4.5, is used to calculate the maximum amount of error-free digital data in bits/s/Hz that can be transmitted with a specified bandwidth in the presence of the noise interference.

$$\frac{C}{B} = \log_2\left(1 + \frac{S}{N}\right)$$

(4.5)

The Shannon Capacity limit may not be attained in practice because of various execution issues. To describe these losses method, a modified Shannon capacity expression for the kth spatial sub-channel and also for the total capacity will be used as,

$$C_k = \frac{\eta_{BW}}{Q}\sum_{q=1}^{Q}\log_2\left(1 + \alpha_{k,q}\beta_{k,q}\eta_{SNR}\frac{S}{N}\right)$$

(4.6)

$$C = \frac{\eta_{BW}}{Q} \sum_{k=1}^{K_q} \sum_{q=1}^{Q} \log_2 \left(1 + \alpha_{k,q} \beta_{k,q} \eta_{SNR} \frac{S}{N} \right) \tag{4.7}$$

ηBW adjusts for the system bandwidth of LTE. η_{SNR} adjusts SNR execution efficiency of LTE.

As stated above, the MIMO is not used in the uplink direction. Therefore, the MIMO is only performed for the downlink direction, the total capacity for the uplink direction is calculated as

$$C = \frac{\eta_{BW}}{Q} \sum_{q=1}^{Q} \log_2 \left(1 + \alpha_{k,q} \beta_{k,q} \eta_{SNR} \frac{S}{N} \right) \tag{4.8}$$

4.2. SNR and Error Probability

The number of waveforms used by the modulator (M) and the duration of these waveforms (T) are concerned by the bit rate of source (R_b).

$$R_b = \frac{\log_2 M}{T} \tag{4.9}$$

The rate in bit/s which may be confirmed by the modulator equals to R_b . The average power spent by the modulator (S) equals to

$$S = \frac{\varepsilon}{T} \tag{4.10}$$

ε gives the average energy of the modulator that signals us. Furthermore, an each signal carries $\log_2 M$ bits. Hence, determining ε_b for the average energy spent is conducted by the modulator to transmit one bit. As a result, $\varepsilon = \varepsilon_b \log_2 M$. The last formula can be defined by the following expression (4.11).

$$S = \varepsilon_b \frac{\log_2 M}{T} = \varepsilon_b R_b \tag{4.11}$$

The proportion between the average signal power and the average noise power are identified as the SNR (symbolically *S/N*). Hence, the last equals $N_0.B_w$. B_w

define the equivalent noise bandwidth of the receiving filter. Therefore, we can have the following expression (4.12).

$$\frac{S}{N} = \frac{S}{N_0 B_w} = \frac{\varepsilon_b}{N_0} \cdot \frac{R_b}{B_w} \tag{4.12}$$

The representation (4.12) demonstrates that the SNR is the goods of two quantities. ε_b/N_0 defines the energy per bit divided by twice the power spectral density. R_b/B_w defines the spectral efficiency of a modulation scheme.

There are three parameters to support the evaluation of a modulation scheme: the bit error probability, $P_b(e)$, the ε_b/N_0 which is necessary to achieve $P_b(e)$, and the bandwidth efficiency R_b/B_w. The first one clarifies the reliability of the transmission, the second calculates the effectiveness in power consuming, and the third measures how influentially the modulation scheme benefits from the bandwidth [24].

The LTE uses the link adaptation based on a good number of MCSs (the Modulation and Coding Set).

The error probability of QPSK may be specified definitively. From [26],

$$P(e) = erfc\left(\sqrt{\frac{\varepsilon_b}{N_0}}\right) - \frac{1}{4}\left[erfc\left(\sqrt{\frac{\varepsilon_b}{N_0}}\right)\right]^2 \tag{4.13}$$

In expression (4.13), $erfc(.)$ is the supplementary error function. A simpler approach for the universal M-ary PSK is to use the upper bound to $P(e)$ [26],

$$P(e) \leq erfc\left(\sqrt{\frac{\varepsilon_b}{N_0} \log_2 M} \sin\frac{\pi}{M}\right), \text{M- PSK} \tag{4.14}$$

The QAM is a linear modulation scheme. Therefore, the source symbols specify the amplitude as well as the phase of a carrier signal. In contrast to the PSK, the signal envelope is unstable. Various QAM families are practical. This study focuses on two considered LTE square constellations with $M = 16$ and $M = 64$. A

simple bound to $P(e)$ being only an approximation that can be useful for large M, will be used for the two modulations [26],

$$P(e) \leq 2erfc\left(\sqrt{\frac{3\log_2 M \; \varepsilon_b}{2(M-1) \, N_0}}\right) \quad , \text{M- QAM} \tag{4.15}$$

Despite an exact maximum BER target, P_b, target with Gray Mapping and expressions (4.12), (4.14) and (4.15), the spectral efficiency, R_b/B, are computed in the function of the SNR as follows;

$$\frac{R_b}{B} = \begin{cases} \dfrac{\log_2 M}{\left(erfc^{-1}(P_{b,target})\right)^2} \sin^2\left(\dfrac{\pi}{M}\right)\dfrac{S}{N} & , \quad M - PSK \\[4mm] \dfrac{3\log_2 M}{2(M-1)\left(erfc^{-1}\left(\dfrac{P_{b,target}\log_2 M}{2}\right)\right)^2}\dfrac{S}{N} & , \quad M - QAM \end{cases} \tag{4.16}$$

Where; B is the transmission bandwidth and considered to be equal to the equivalent noise bandwidth, B_w.

4.3. Bandwith Efficiency Calculation

The LTE bandwidth efficiency,η_{BW}, is reduced by various issues which are defined below.

4.3.1. ACLR Overheads

The bandwidth occupancy is diminished because of the restrictions of ACLR. Being described as the ratio and the transmitted power to the power measured afterwards a receiver (RX) filter in the adjacent radio-frequency channel, the ACLR is a measurement of the transmitter (TX) performance for wideband networks, In consideration of the parameters for LTE downlink transmission scheme, the bandwidth efficiency related to the ACLR, η_{ACLR} is computed as,

$$\eta_{ACLR} = \frac{(N_{SC}^{DL} - 1)\,\Delta f}{B} = 0.9 \tag{4.17}$$

Where; N_{SC}^{DL} is the number of downlink data subcarriers, Δf is the subcarrier bandwidth. Considering a 5 MHz bandwidth channel, it has 25 resource blocks. In case that all the bandwidth is used for downlink transmission, $N_{SC}^{DL} = 300$, and $\Delta f = 15$ kHz in LTE, insert these values into (4.17) gives $\eta_{ACLR} = 0.897 \approx 0.9$.

4.3.2. OFDM Symbol Structure with Cyclic Prefix Overheads

Figure 17 demonstrates the structure of an OFDM symbol. A cyclic prefix is inserted at the beginning of the OFDM symbol with the time period T_{cp}, and T_u is a useful symbol time period. The total length of an OFDM symbol is the sum of T_{cp} and T_u. Hence, the bandwidth efficiency related to the cyclic prefix overhead, η_{CP}, needs to be considered.
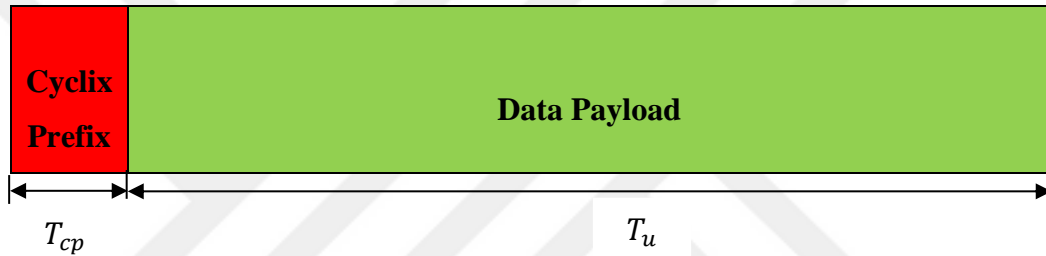
Figure 17 Structure of an OFDM symbol

$$\eta_{CP} = 1 - \frac{T_{slot} - N_{symb}^{DL} T_u}{T_{slot}} = \frac{N_{symb}^{DL} T_u}{T_{slot}} \tag{4.18}$$

Where; T_{slot} is one time slot of an OFDM symbol and is equal to 0.5 ms. $\Delta f = 15$ kHz is the subcarrier space in LTE. T_u is calculated as $T_u = 1/\Delta f \approx 66.7$ μs. The value N_{symb}^{DL} can be found in Table 7. For the Normal Cyclic Prefix, $\eta_{CP} = 0.93$ and for the Extended Cyclic Prefix, $\eta_{CP} = 0.80$. In addition, these results are applied for the UP direction in LTE.

4.3.3. Reference Signals Overheads

As put forth in Section 3.4.3., reference symbols are inserted into the OFDM/SCFDM transmission. The density of the reference symbols consists in the number of T_x antennas in use in the MIMO configuration as presented in Figure 18 (one antenna, two antennas and four antennas configurations, respectively),
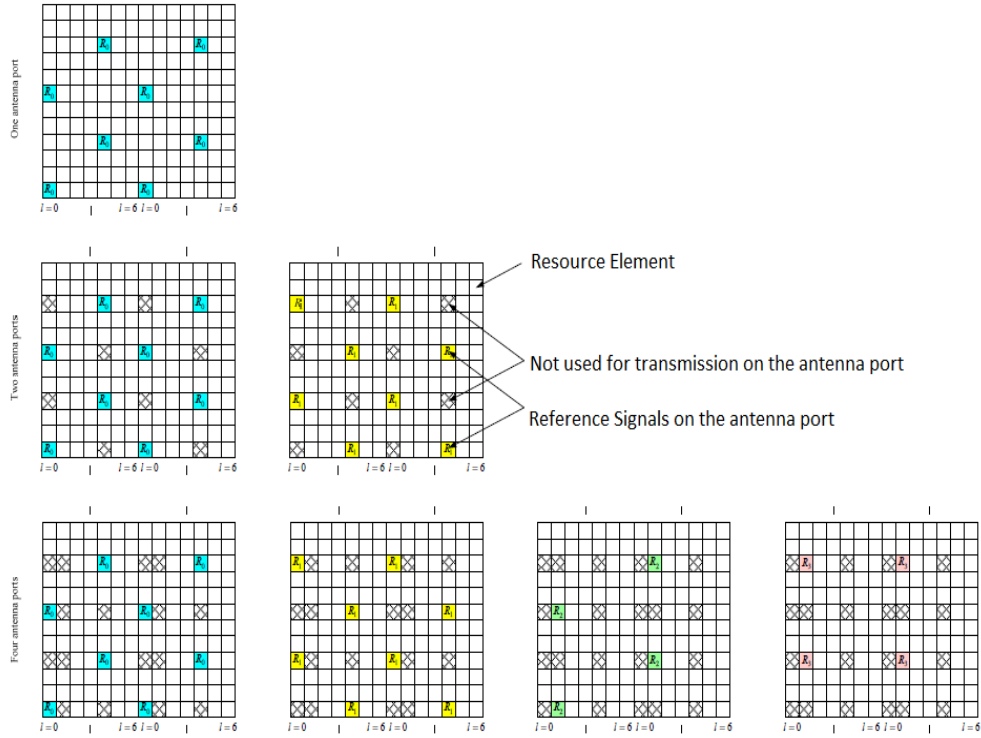
Figure 18 Downlink Reference Signal structure with normal cyclic prefix [18]

Therefore, the bandwidth efficiency η_{RS_DL} that results fromthe reference symbol addition using r T_x antennas is

$$
\eta_{RS\_DL} = \begin{cases} 1 - \dfrac{4r}{N_{SC}^{RB} N_{symb}^{DL}} = 1 - \dfrac{r}{21} & r = 1,2 \\[4mm] 1 - \dfrac{2r + 4}{N_{SC}^{RB} N_{symb}^{DL}} = 1 - \dfrac{r + 2}{42} & r = 3,4 \end{cases} \tag{4.19}
$$

Where; N_{SC}^{RB} and N_{symb}^{DL} (N_{symb}^{UL}) are 12 subcarriers per resource block and 7 OFDM symbols per subcarrier [24].

As presented in Figure 19, a reference symbol is transmitted within the fourth symbol of each uplink slot for the uplink direction.
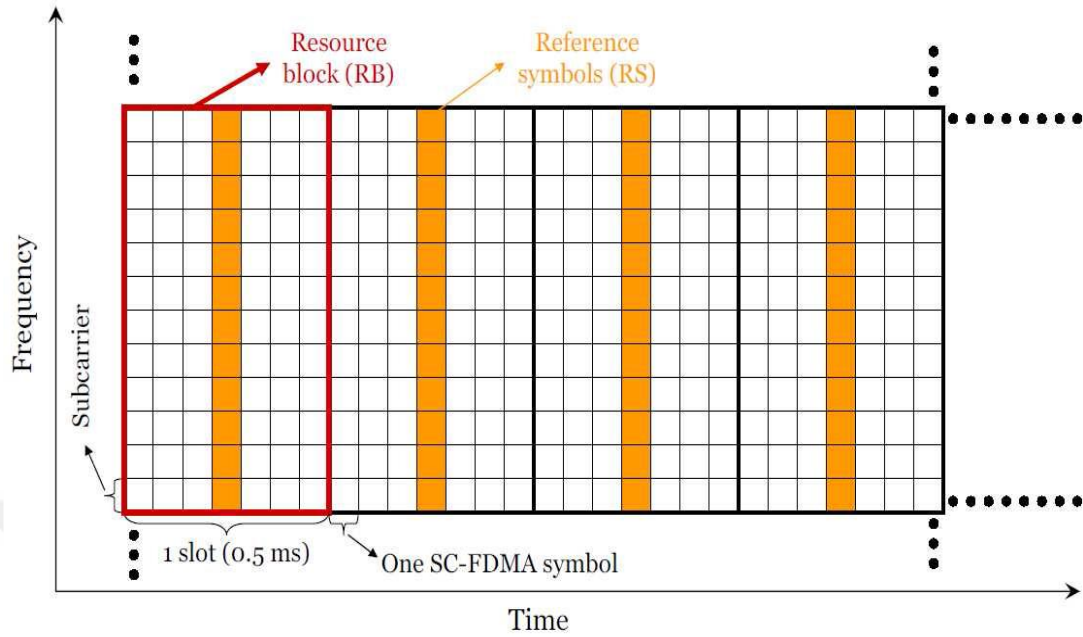
Figure 19 Uplink Reference Signal structure with normal cyclic prefix [23]

The bandwidth efficiency η_{RS_UL} may be computed as

$$\eta_{RS\_UL} = 1 - \frac{N_{SC}^{RB}}{N_{SC}^{RB} N_{symb}^{UL}} = 1 - \frac{1}{N_{symb}^{UL}} \approx 0.86 \tag{4.20}$$

4.3.4. Synchronization Signal Overheads

Two synchronization signals (see Section 3.5), being the Primary Synchronization Signal (PSS) and the Secondary Synchronization Signal (SSS) are used in the synchronization procedure for both FDD and TDD mode, as illustrated in Figure 20 and Figure 21.
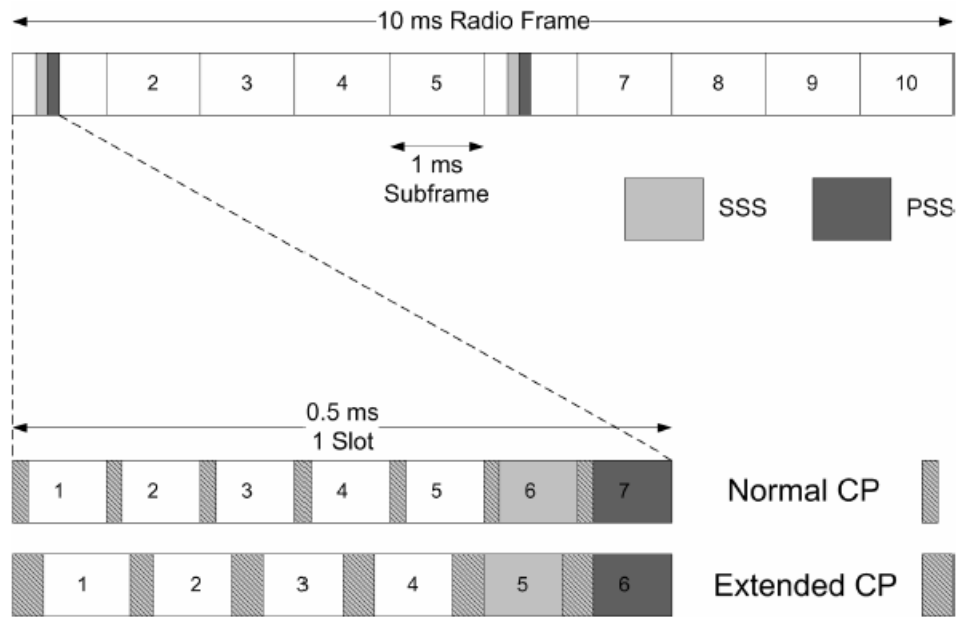
Figure 20 PSS and SSS frame and slot structure in time domain in the FDD case [9]
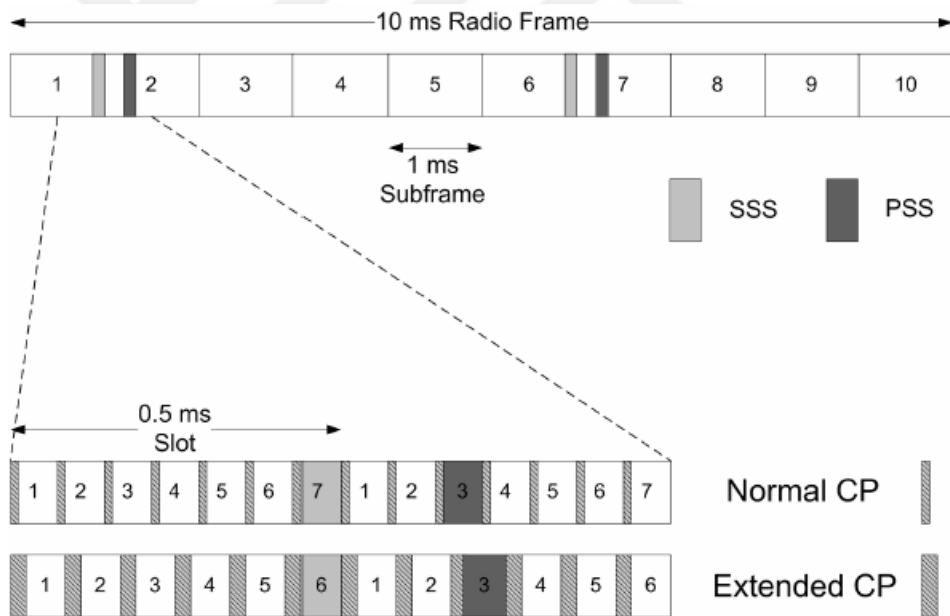
Figure 21 PSS and SSS frame and slot structure in time domain in the TDD case [9]

Figure 22 demonstrates the mapping of the PSS and SSS to subcarriers in the frequency domain.
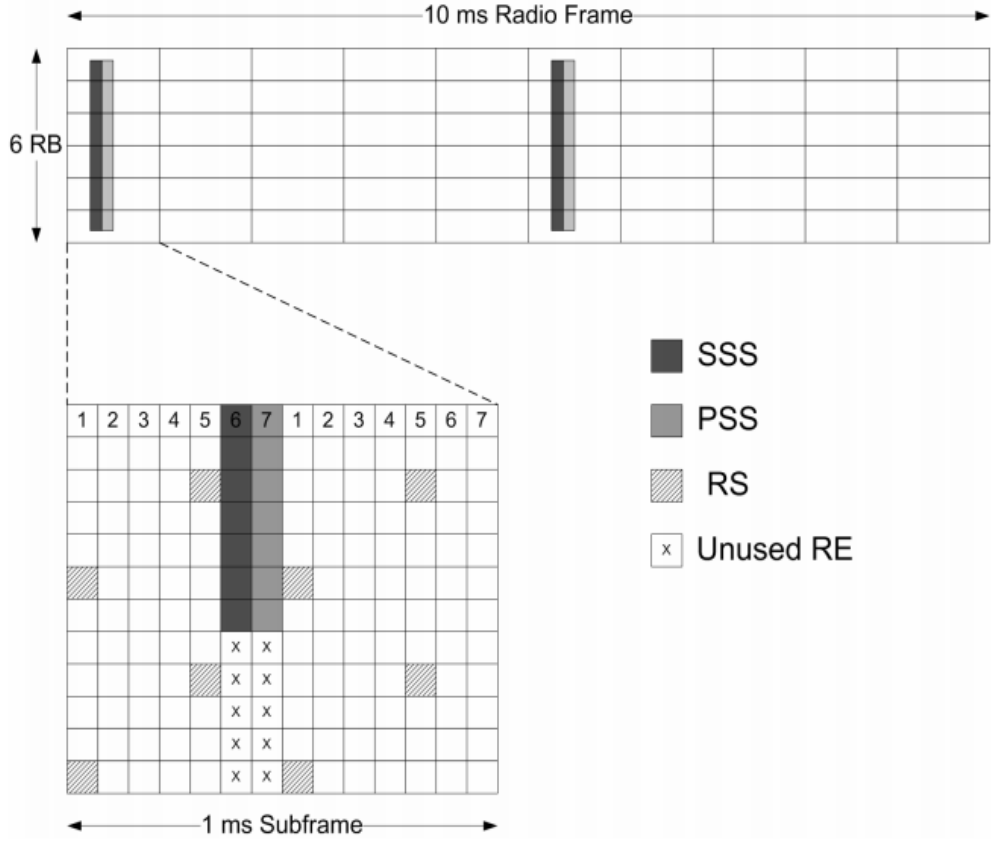
Figure 22 PSS and SSS frame structure in frequency and time domain [9]

According to Figure 22, there are four OFDM symbols per 10 ms Radio Frame for both FDD and TDD for the synchronization signals. The PSS and SSS are transmitted in the central six resource blocks by offering the frequency mapping of synchronization signals to be constant with the system bandwidth. Each of the PSS and SSS consists of a sequence of length 62 symbols and is mapped to the central 62 subcarriers. Five resource elements taking place at each end of every one synchronization sequence are not used. Therefore, the bandwidth efficiency related to the synchronization signals overheads including the unused resource elements, η_{Sync_DL}, is given by

$$\eta_{Sync\_DL} = 1 - \frac{4 \times 6 \times N_{SC}^{RB}}{20 \times n \times N_{SC}^{RB} N_{symb}^{DL}} = 1 - \frac{6}{35n} \qquad n = 6,15,25,50,75,100 \qquad (4.21)$$

Where; $N_{symb}^{DL} = 7$ and n is the number of resource blocks for the bandwidths that LTE supports. The mapping between the n and the bandwidths can be found in Table 6.

34

4.3.5. PBCH Overheads

As presented in Section 3.6, the PBCH is used to carry the Master Information Block and to broadcast the system information to the whole network.
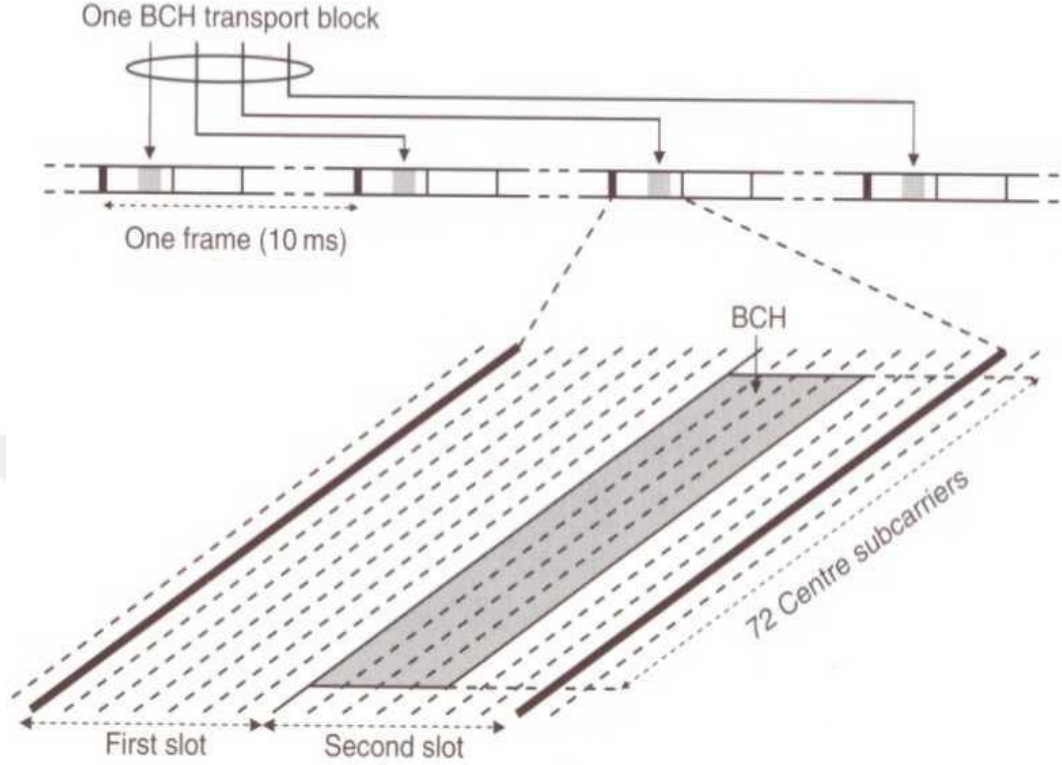
Figure 23 PBCH structure [20]

As presented in Figure 23, the PBCH is transmitted within the first four OFDM symbols of the second slot in the sub-frame 0 and only over the 72 center subcarriers in each radio frame without regard to the current bandwidth of the system. Therefore, the bandwidth efficiency related to the PBCH overheads, η_{BCH_DL}, is presented in equation (4.22).

$$\eta_{BCH\_DL} = 1 - \frac{72 \times 4}{20 n N_{SC}^{RB} N_{symb}^{DL}} = 1 - \frac{6}{35n} \tag{4.22}$$

Where; n (6, 15, 25, 50, 75, 100) is the number of resource blocks for the used bandwidths. The mapping between n and the bandwidths can be found in Table 6.

4.3.6. Random Access Preamble Overheads

The initial step of a Contention-based procedure is the transmission of a random access preamble as described in Section 3.7. The time-frequency resource

which the random access preamble is transmitted on is also known as the Physical Random Access Channel (PRACH). A sub-frame is reserved for the preamble transmissions as the basic time unit is 1ms for data transmission in LTE. In the reserved resources, the random-access preamble is transmitted as presented in Figure 24.
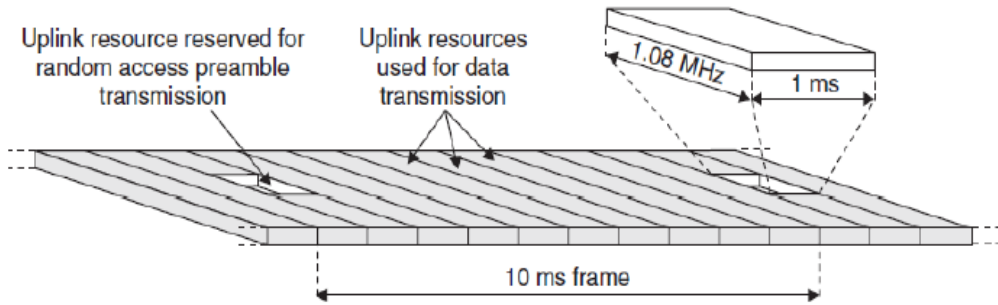
Figure 24 Principal illustration of random access preamble transmission [20]

In the frequency domain, there is a bandwidth of six resource blocks (1.08 MHz) included in the random-access preamble. This theoretically matches with the smallest bandwidth where LTE may operate with six resource blocks. In this sense, the same random-access preamble structure can be used irrespective of the transmission bandwidth in the cell. Because larger spectrum allocations provide an improved random access capacity. Therefore, the PRACH overheads are based on the operating bandwidth. In this thesis, the assumption was made upon the presence of one random access preamble in every 10 ms radio frame. The bandwidth efficiency related to PBCH overheads, η_{RAP_UL}, is thus

$$\eta_{RAP\_UL} = 1 - \frac{6 \times 2N_{SC}^{RB} N_{SYMB}^{UL}}{20 n N_{SC}^{RB} N_{SYMB}^{UL}} = 1 - \frac{3}{5n} \qquad (4.33)$$

Where; n (6, 15, 25, 50, 75, 100) is the number of resource blocks for the used bandwidths. The mapping between the n and the bandwidths can be found in Table 6.

4.3.7. L1/L2 Layer Control Signal Overheads

Downlink and uplink control signaling channels are needed for the transmission of downlink and uplink transport channels. This control signaling is

usually referred to as the downlink and uplink L1/L2 control signaling, which displays the knowledge partially originated from the physical layer and MAC layer.

In the downlink direction, the control signaling overheads are related to the transmission of the downlink transport channels such as the DLSCH transmission. The downlink L1/L2 control signaling is transmitted within the first part of each 1 ms sub-frame. 3 OFDM symbols within one sub-frame (1ms) are occupied by the L1/L2 control signaling. Downlink L1/L2 control signaling bandwidth efficiency is like in expression (4.34) [24].

$$\eta_{L1/L2\_DL} = 1 - \frac{3N_{SC}^{RB}}{2N_{SC}^{RB}N_{symb}^{DL} - 2r} \approx 0.78 \quad r = 1,2,,3,4 \tag{4.34}$$

Where; r is the number of T_x antennas.

The L1/L2 control signaling overheads are engaged in Physical Uplink Shared Channel (PUSCH) and Physical Uplink Control Channel (PUCCH) for the uplink direction. The first one carries the UL traffic data while the latter carries the uplink control information. In this thesis, solely the L1/L2 control signaling overheads in the PUCCH are considered for the convenience.
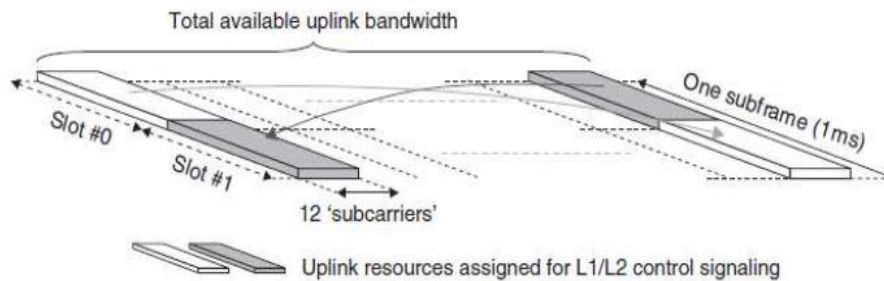
Figure 25 Resource structure to be used for uplink L1/L2 control signaling on PUCCH [20]

Figure 25 demonstrates how one L1/L2 control signaling includes 12 subcarriers (one resource block) in the upper part of the spectrum in the first slot of a sub-frame and an equal sized resource in the lower part of the spectrum during the second slot of the sub-frame or vice versa. Therefore, the bandwidth efficiency $\eta_{L1/L2\_UL}$ is based on the transmission bandwidths and may be calculated as follows;

$$\eta_{L1/L2\_UL} = 1 - \frac{2N_{SC}^{RB}N_{symb}^{UL}}{2nN_{SC}^{RB}N_{symb}^{UL}} = 1 - \frac{1}{n} \tag{4.35}$$

Where; n (6, 15, 25, 50, 75, 100) is the number of the resource blocks for the used bandwidths. The mapping between the n and the bandwidths can be found in Table 6. On condition that higher number of resources is required for the uplink L1/L2 control signaling, as in case of a great amount of general transmission bandwidth supporting many users, the additional resource blocks may be assigned next to the previously assigned resource blocks. It generally uses from 1 to 6 resource blocks overheads [5].

4.3.8. Summary of the Bandwidth Efficiency

The overheads calculated for the bandwidth efficiency from section 4.3.1 to section 4.3.3 are related to the link level efficiency. From section 4.3.4 to section 4.3.7, the system level overheads are taken into consideration.

The total result expressions for the LTE link-level and system-level both downlink and uplink bandwidth efficiency are like those between (4.36) and (4.39).

$$\eta_{BW\_DL\_LIK} = \eta_{ACLR} \times \eta_{CP} \times \eta_{RS\_DL} \tag{4.36}$$

$$\eta_{BW\_DL\_SYS} = \eta_{ACLR} \times \eta_{CP} \times \eta_{RS\_DL} \times \eta_{Sync\_DL} \times \eta_{BCH\_DL} \times \eta_{L1/L2\_DL} \tag{4.37}$$

$$\eta_{BW\_UL\_LIK} = \eta_{CP} \times \eta_{RS\_UL} \tag{4.38}$$

$$\eta_{BW\_UL\_SYS} = \eta_{CP} \times \eta_{RS\_UL} \times \eta_{RAP\_UL} \times \eta_{BCH\_DL} \times \eta_{L1/L2\_UL} \tag{4.39}$$

$\eta_{BW\_DL\_LIK}$: Downlink link-level bandwidth efficiency.

$\eta_{BW\_DL\_SYS}$: Downlink system-level bandwidth efficiency.

$\eta_{BW\_UL\_LIK}$: Uplink link-level bandwidth efficiency

$\eta_{BW\_UL\_SYS}$: Uplink system-level bandwidth efficiency

For instance, when the system bandwidth is considered to be 10 MHz with the normal Cyclic Prefix (CP), the bandwidth efficiency results are displayed in Table 8 for downlink and Table 9 for the uplink.

Bandwidth Efficiency	Number of Tx antennas (r)			
	1	2	3	4
η_{ACLR}	0.9			
η_{CP}	0.93			
η_{RS_DL}	0.95	0.90	0.89	0.86
η_{Sync_Dl}	0.99			
η_{BCH_DL}	0.99			
$\eta_{L1/L2\_DL}$	0.78			
$\eta_{BW\_DL\_LIK}$	0.80	0.76	0.75	0.72
$\eta_{BW\_DL\_SYS}$	0.62	0.59	0.58	0.56

Table 8 The Bandwidth Efficiency results for the DL with MIMO configuration for LTE [24]

Bandwidth Efficiency	Result
η_{CP}	0.93
η_{RS_UL}	0.86
η_{RAP_UL}	0.99
$\eta_{L1/L2\_UL}$	0.98
$\eta_{BW\_UL\_LIK}$	0.80
$\eta_{BW\_UL\_SYS}$	0.78

Table 9 The Bandwidth Efficiency results for the UL for LTE

4.4. SNR Efficiency Calculation

The spectral efficiency performance which uses the coded modulation schemes can be estimated by means of the previous inputs. As described in the equation (4.16), the LTE spectral efficiency with the coded QPSK (M=4), 16-QAM ($M = 16$) and 64-QAM ($M = 64$) is, [24]

$$\frac{R_b}{B} = min\left(\frac{3\log_2 M \frac{n}{k} G_{MCS}(P_{b,target})\frac{S}{N}}{2(M-1)\left(erfc^{-1}\left(\frac{P_{b,target}\log_2 M}{2}\right)\right)^2}, \ \frac{k}{n}\log_2 M\right) \qquad (4.40)$$

The given MCS requires a certain SNIR (measured at the rx antenna) in order to be able to operate with an adequately low BER in the output data. An MCS with a higher throughput needs a higher SNIR for the operation. AMC operates by means of measuring and feeding back the channel SNIR to the transmitter, which selects a proper MCS from a "codeset" to maximize the throughput at that SNIR subsequently. A code set, which is designed to cover a range of SNRs, includes a good number of MCSs. Figure 26 presents an instance of a codeset in which each MCS includes the highest throughput for a 1-2dB range of SNIR [27].
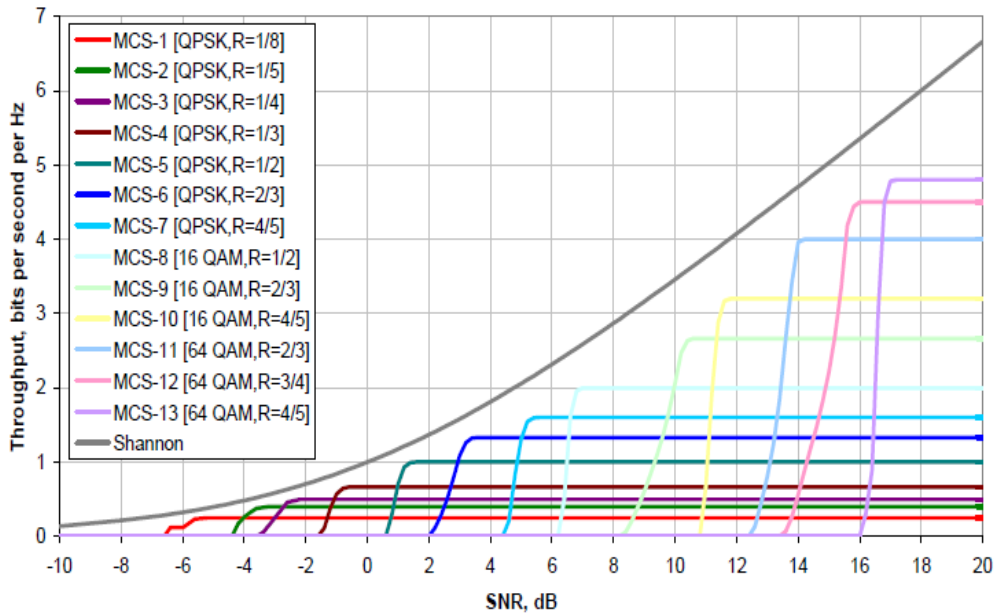
Figure 26 Throughput of a set of Coding and Modulation Combinations in LTE [27]

Figure 26 presents the Shannon bound indicating the utmost theoretical throughput to be obtained over an AWGN channel with a given SNR.

As presented in Figure 27, it is possible to approximate the spectral efficiency with an attenuated and truncated form of the Shannon bound.
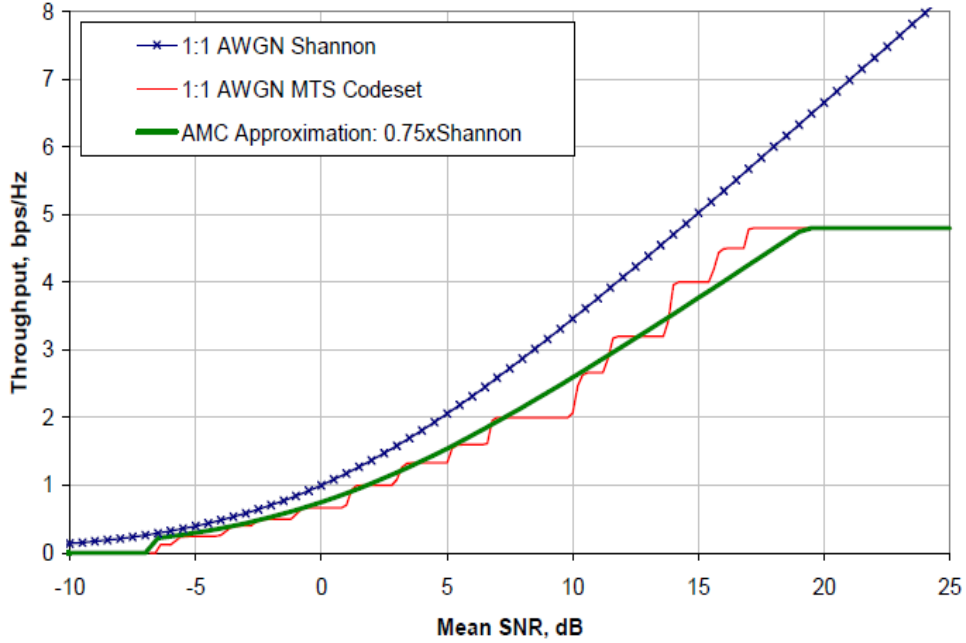
Figure 27 Approximating AMC with an attenuated and truncated form of the Shannon Bound [27]

The results for the curve fitting correlation and $\eta_{SNR,r}$ computing are offered in Table 10.

Nr. Of TX antenna, r	$\eta_{BW,r}$	$\eta_{SNR,r}$	Correlation Coef.
1	0.80	**0.91**	0.9954
2	0.76	**1.05**	0.9947
3	0.75	**1.11**	0.9943
4	0.72	**1.24**	0.9930

Table 10 SNR Efficiency Computing [24]

4.5. MIMO CAPACITY

As presented in Figure 26, the SNR efficiency graph was calculated according to 1x1 SISO (Single Input Single Output) antenna structure. Power in parallel channels was calculated by water-filling algorithms and plotted as presented in Figure 28 after the MIMO (Multiple Input Multiple Output) channel capacity was modeled with nt transmitter, nr receiver antenna structures, and Rayleigh Fading channels. In different circumstances, MIMO derived a profit in the ratio of 70% with

2x2 antenna structures, 100% with 2x3 and 3x2 antenna structures, and 205% with 4x4 antenna structures [28].
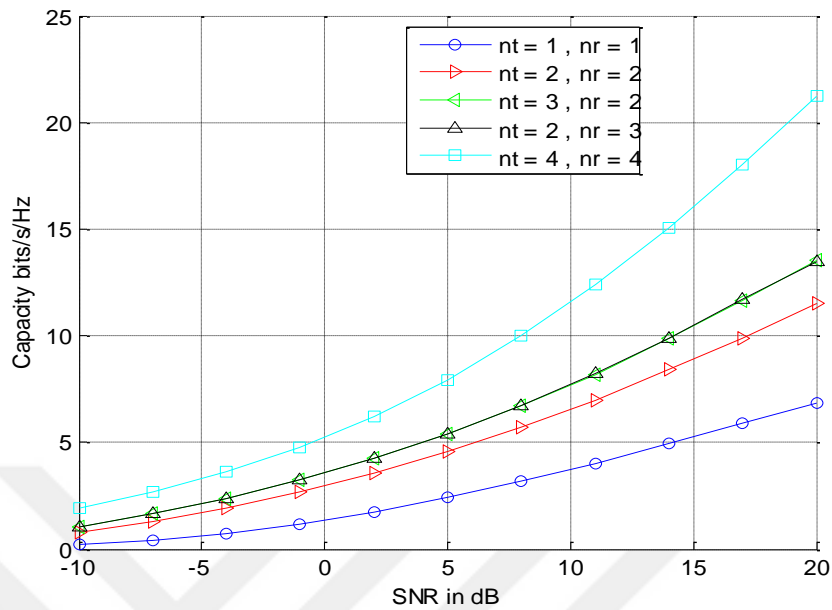
Figure 28 MIMO Capacity [28]

4.6. Network Sizing

This section is confined to how the cell throughput values are transformed into the maximum number of broadband subscribers. To this end, Table 11 presents two different suggested methods. The first one is a traffic volume based method while the other is based on data rate. The traffic volume based approach estimates the maximum traffic volume in gigabytes that might be carried by LTE 20 MHz 1 + 1 + 1 configuration. The spectral efficiency is presumed to be 1.74 bps/Hz/cell using 2 x 2 MIMO [10].

Traffic Volume Based Dimensioning		Data Rate Based Dimensioning	
Cell Capacity 35 Mbps	20MHz x 1.74 bps/Hz/cell	Cell Capacity 35 Mbps	From simulations
Convert Mbps to GBytes	/ 8192	Busy hour average loading 50 %	x 50%
3600 seconds per hour	x 3600	Required user data rate	/ 1Mbps
Busy hour average loading 50%	x 50%	Overbooking factor	/ 20
Busy hour carries 15% of daily traffic	/15%	Average busy hour data rate per sub	= 50 kbps
30 days per month	x 30	3 sectors per site	x3
3 sectors per site	x 3 ⇒ 4600 GB /site/month	Total	1050 subs/ site
5GB traffic per user	/5 GB		
Total	920 subs/site		

Table 11 LTE dimensioning example [10]

As presented in Table 11, 15% of the daily traffic is presumably carried by the busy house and the average loading of the busy hour is 50%. The loading depends on the targeted data rates along the busy hour; when the loading is higher, all the data rates are lower. In addition, the maximum loading depends on the applied QoS differentiation strategy: QoS differentiation approximates the loading value to 100% while the data rates are sustained for more significant connections at the same time.

Another approach presumes an objective of 1 Mbps per subscriber. Since only a few the subscribers download data simultaneously, an overbooking factor

such as 20 can be applied. In this case the average data rate of the busy hour is 50 kbps per subscriber and a total of 1050 subscribers use this case per site

According to this calculation, LTE is capable of providing support to a good number of broadband data subscribers.

The terminal categories are presented in Table 12.

	Category 1	Category 2	Category 3	Category 4	Category 5
Peak rate downlink (approximately)	10 Mbps	50 Mbps	100 Mbps	150 Mbps	300 Mbps
Peak rate uplink (approximately)	5 Mbps	25 Mbps	50 Mbps	50 Mbps	75 Mbps
Max bits received within TTI	10296	51024	102048	150752	299552
Max bits transmitted within TTI	5160	25456	51024	51024	75376
RF bandwidth	20 MHz	20 MHz	20 MHz	20 MHz	20 MHz
Modulation downlink	64 QAM	64 QAM	64 QAM	64 QAM	64 QAM
Modulation uplink	16 QAM	16 QAM	16 QAM	16 QAM	64 QAM
Receiver diversity	Yes	Yes	Yes	Yes	Yes
eNodeB diversity	1-4 tx	1-4 tx	1-4 tx	1-4 tx	1-4 tx
MIMO downlink	Optional	2 x 2	2 x 2	2 x 2	4 x 4

Table 12 Terminal Categories [10][29]

CHAPTER 5

5. COVERAGE CALCULATIONS at LTE

The access of the LTE network's subscribers to the offered services without any interruptions depends on the network coverage. Therefore, the coverage calculations have an important place in cell planning. For accessing to a projected service, assumed system parameters and necessary source requirement coverage calculations are found.

5.1. Path loss Calculations

Path loss is an attenuation with various influences of output signal from base station until it reaches a user's equipment. It is the base parameter of cell radius calculation. Due to different geographical features and environmental factors, path loss does not have a single statement, yet has a lot of empirical statements based on experimental measurements. In this section, we analyzed TS 36.942 model proposed for the LTE of 3GPP and compressed Extended Hata and Walfish-Ikegami models. [27][6]

When TS 36.942 model is examined, macro cell propagation model formula for urban area is indicated in the equation (5.1). [30]:

$$L = 40 \cdot (1 - 4 \cdot 10^{-3} \cdot Dhb) \cdot \log_{10}(R) - 18 \cdot \log_{10}(Dhb) + 21 \cdot \log_{10}(f) + 80 dB \qquad (5.1)$$

where:

R is the base station-UE separation in kilometers

f is the carrier frequency in MHz

Dhb is the base station antenna height in meters, measured from the average rooftop level.

Considering a carrier frequency of 900MHz and a base station antenna with the height of 15 meters above the average rooftop level, the propagation model can be formulated as follows (5.2):

$$L = 120,9 + 37,6 \log_{10}(R) \tag{5.2}$$

Considering a carrier frequency of 2000MHz and a base station antenna with the height of 15 meters above the average rooftop level, the propagation model can be formulated as follows (5.3):

$$L = 128,1 + 37,6 \log_{10}(R) \tag{5.3}$$

In rural area, the Hata model, which was used in the work item UMTS900 [31], can be used once again:

$$L(R) = 69.55 + 26.16 \log_{10}(f) - 13.82 \log_{10}(Hb) + [44.9 - 6.55 \log_{10}(Hb)] \log(R) \tag{5.4}$$
$$- 4.78(\log_{10}(f))^2 + 18.33 \log_{10}(f) - 40.94$$

where:

Hb is the base station antenna height above the ground in meters

Considering a carrier frequency of 900MHz and a base station antenna with the height of 45 meters above the ground, the propagation model can be formulated as follows (5.5):

$$L = 95,5 + 34,1 \log_{10}(R) \tag{5.5}$$

Following the calculation of L, log-normally distributed shadowing (LogF) with standard deviation of 10dB needs to be added [31], [30]. A Shadowing correlation factor of 0.5 for the shadowing between sites (regardless of the aggressing or victim system) and of 1 between sectors of the same site needs to be used. These models are valid for the Non-line-of-sight (NLOS) case only, and obtained for distance few hundred meters to kilometers of the cell radius. For places almost uniform of building length, they are applicable. The path loss can be formulated as follows (5.6):

$$Pathloss\_macro\ (PL) = L + Log\ F \qquad\qquad (5.6)$$

The calculated path loss value with respect to separation distance is presented in Figure 29. The sensitivity of the path loss models regarding the frequency is demonstrated in Figure 30. [6]
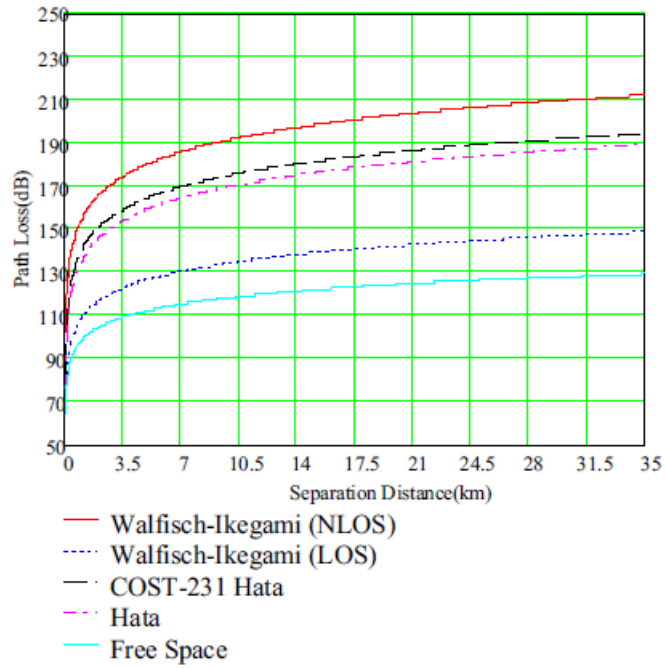
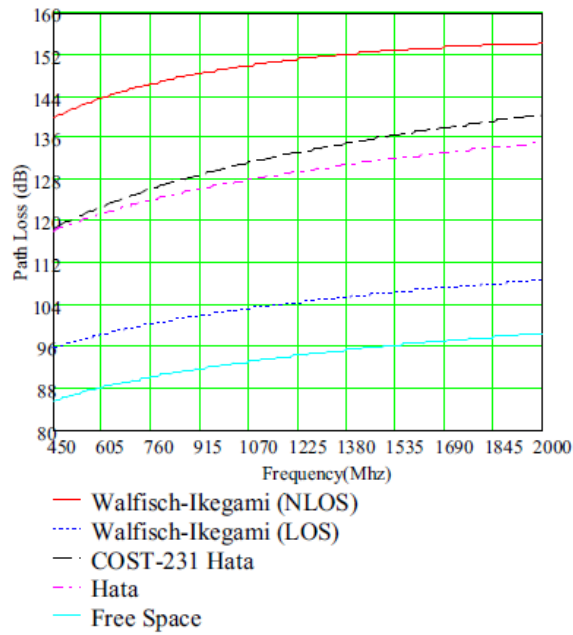**Figure 29** Comparisons of Path Losses [6]

Figure 30 Path Loss versus frequency [6]

5.2. Link Budget Calculations

A link budget refers to accounting all gains and losses of the output signal from the transmitter until the signal reaches to receiver in all systems which can be communicated with Radio Frequency (RF). The link budgets find the cell radius and capacity areas.

A link budget refers to accounting all of the gains and losses obtained from the transmitter, through the medium to the receiver in a radio system. A link budget equation in the wireless channel is displayed in formula (5.7).

$$P_{Rx} = P_{Tx} + G_{Tx} + G_{Rx} - L_{Tx} - L_{Rx} + PM - PL \qquad (5.7)$$

Where; P_{Rx} is the received power (dBm). P_{Tx} is the transmitter output power (dBm). G_{Tx} is the transmitter antenna gain (dBi). G_{Rx} is the receiver antenna gain (dBi). L_{Tx} and L_{Rx} are the cable and other losses on the transmitter and receiver side (dB), sequentially. PM refers to the planning margin and PL to the path loss (dB). A planning margin between 10 and 25 dB is added to the accounting for the necessary received signal allowance for fading, prediction errors and additional losses.

48

In order to compute the maximum coverage, the minimum received power P_{Rx} is considered. In LTE, the Reference Sensitivity Level is the minimum mean received signal strength applied to two of the antenna ports where sufficient SINR can be found for the specified modulation scheme in order to fulfill a minimum throughput requirement of 95% of the maximum possible [9].

REFSENS [9] is a range of values which can be computed as in the equation (5.8).

$$REFSENS = kTB + NF + SINR + IM - G_d \qquad (5.8)$$

kTB represents the Thermal Noise Level in a specified noise bandwidth B, where $B = N_{RB} \times 180$ kHz in LTE and N_{RB} is the number of RBs and 180 kHz is the bandwidth of one RB. The kTB can be calculated as

$$kTB = KT + 10\log_{10}(N_{RB} \times 180kHz) \qquad (5.9)$$
$$= -174(dBm/Hz) + 10\log_{10}(N_{RB} \times 180kHz)$$

The Noise Figure (NF) refers to the measure of the degradation in the SINR which results from the components in the RF signal chain. LTE in the 3GPP standards defines a NF requirement of 9 dB for the UE. The Implementation Margin (IM) is called the placement tolerance, and refers to the value between 2 dB and 4 dB.

Graphics for incident power (*Prx*) reaching the receiver in equality (5.7) by the using parameters listed in Table 13 are like those in Figure 31 and Figure 32 and there graphics were plotted based on the distance for 900 MHz and 2000MHz.

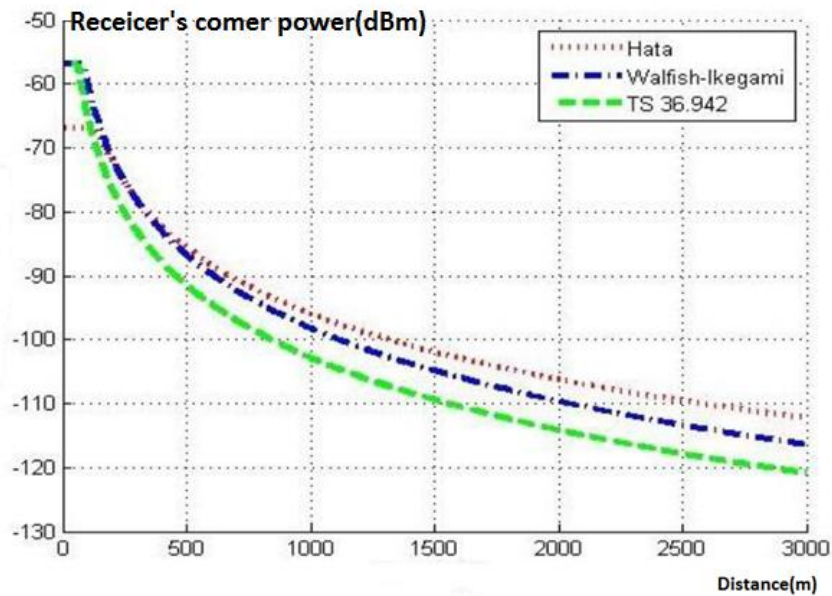| Parameter	Value
Transmitter antenna gain (G_{Tx})	15dBi
Transmitter output power(P_{Tx})	43dBm
Base Station Noise Factory(F)	5dB
Receiver antenna gain (G_{Rx})	0dBi
Minimum coupling loss(MCL)	70dB
Base station antenna height above ground(Hb)	45m
Base station antenna height(Dhb)	15m
User equipment antenna height(Hm)	1.5m

Table 13 Using parameters

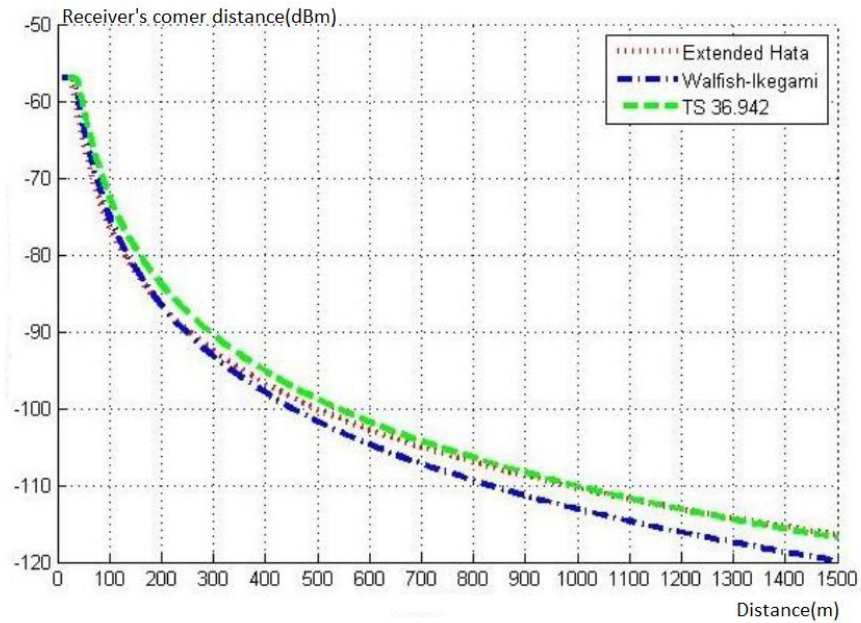**Figure 31** 900 MHz micro cell urban area's coming receiver power graph

Figure 32 2000 MHz micro cell urban area's coming receiver power graph

When receiver sensitivity, REFSENS, is taken -110 dBm, the average cell radiuses in the given frequencies can be illustrated as in Table 14.

Carrier Frequency	Using Models		
	Extended Hata	Walfish-Ikegami	TS 36.942
900 MHz	2500m	2000m	1500m
2000MHz	1000m	850m	1000m

Table 14 Calculated Cell Radiuses

5.3. Interference Coordination and Frequency Reuse

The inter-cell interference is the most important problem for the system throughput performance in cellular networks for cell edge users. The inter-cell interference system performance is limited in all cellular networks with a frequency reuse factor of one as the performance of the communicating users in the cell edge decreases. In this sense, it can be asserted that the management of the inter-cell interference has a more significant role.

The scheduling strategy of the eNodeB is to be found as an element of the inter-cell interference coordination. Hence, the user data rates at the cell edge may increase when the interference is kept at certain limits [9].

51

The impact of the inter-cell interference on the users is investigated with an analytic method. In case that a user k has no experience with any interference, its accessible rate in a RB m of subframe f may be expressed as

$$R_{k,no-Int(m,f)} = \frac{B}{M}\log\left[1 + \frac{P^s(m,f)|H_k^s(m,f)|^2}{N_0}\right] \qquad (5.10)$$

Where; $H_k^s(m,f)$ refers to the channel gain from the serving cell s for the user k, $P^s(m,f)$ to the transmit power from cell s and N_0 to the noise power. When the neighboring cells transmit in the same time-frequency resources, the achievable rate for user k is reduced to

$$R_{k,Int}(m,f) = \frac{B}{M}\log\left[1 + \frac{P^s(m,f)|H_k^s(m,f)|^2}{N_0 + \sum_{i\neq s}P^i(m,f)|H_k^i(m,f)|^2}\right] \qquad (5.11)$$

Where; the indices i refer to the interfering cells.

Thereafter, the rate loss for the user k may be expressed as in the equation below (5.12).

$$R_{k,loss}(m,f) = R_{k,no-Int}(m,f) - R_{k,Int}(m,f) \qquad (5.12)$$

$$= \frac{B}{M}\log\left\{\frac{1+SNR}{1+\left[\frac{1}{SNR} + \frac{\sum_{i\neq s}P^i(m,f)|H_k^i(m,f)|^2}{P^s(m,f)|H_k^s(m,f)|^2}\right]^{-1}}\right\}$$

For the user k, Figure 33 displays the rate loss as a function of the total inter-cell interference to signal ratio
$\alpha = \left[\left(\sum_{i\neq s}P^i(m,f)|H_k^i(m,f)|^2\right)/(P^s(m,f)|H_k^s(m,f)|^2)\right]$,
with SNR =0 dB. Which level of interference is equal to the required signal level (i.e. $\alpha \approx 0$ dB) can be clearly observed as the user k experiences a rate loss at the rate of nearly 40%. As presented in Figure 33, the data losses of the communicating users

at cell edges increase in parallel with each other when the inter-cell interference increases.

With the purpose of revealing a further importance of the interference and power allocation based on the system configuration, we analyzed two instances of a cellular system with two cells (*s*1 and *s*2) and one active user per cell (*k*1 and *k*2 respectively). Each user receives the required signal from its serving cell as the inter-cell interference comes from the other cell.

Figure 34(a) presents that each user is located close to its respective eNodeB. Because of the fact that the users are close to the cell center, the neighboring cell-interference power is much lower than the serving cell signal power

$$\left(\left| H_{k_1}^{s_1}(m,f) \right| \gg \left| H_{k_2}^{s_2}(m,f) \right| \text{ and } \left| H_{k_2}^{s_2}(m,f) \right| \gg \left| H_{k_2}^{s_1}(m,f) \right| \right).$$

Therefore, the data losses are not a matter of discussion at this point.

Figure 34(b)) presents that the users are now located near the edge of their respective cells. In such a case, the neighboring cell- interference power is close to each other in comparison to the serving cell signal power

$$\left(\left| H_{k_1}^{s_1}(m,f) \right| \approx \left| H_{k_1}^{s_2}(m,f) \right| \text{ and } \left| H_{k_2}^{s_2}(m,f) \right| \approx \left| H_{k_2}^{s_1}(m,f) \right| \right).$$

The capacity of the system with two eNodeBs and two users can be demonstrated through the equation as below (5.13).

$$R_{Tot} = \frac{B}{M} \left(\log\left(1 + \frac{P^{s_1} \left| H_{k_1}^{s_1}(m,f) \right|^2}{N_0 + P^{s_2} \left| H_{k_1}^{s_2}(m,f) \right|^2} \right) + \log\left(1 + \frac{P^{s_2} \left| H_{k_1}^{s_2}(m,f) \right|^2}{N_0 + P^{s_1} \left| H_{k_2}^{s_1}(m,f) \right|^2} \right) \right) \qquad (5.13)$$
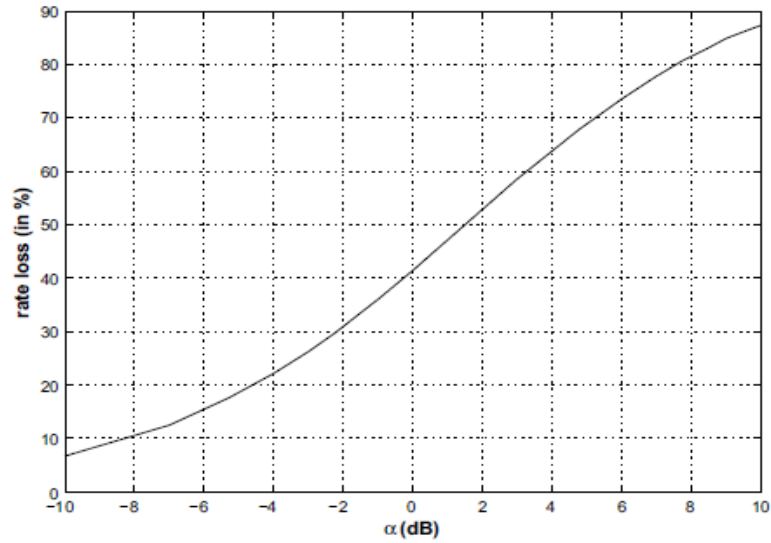
Figure 33 User's rate loss because of interference [9]

Each cell may be divided into two parts, as the inner part and the outer part. A frequency reuse factor of 1 can be applied in the inner part which the users ezperimentation a low level of interference in and requires less power to communicate with the serving cell as well. On the other hand, scheduling restrictions are applied in the outer part, as follows. The neighboring cells may transmit solely at low power (probably to users in the inner parts of the neighboring cells) with the purpose of avoiding any powerful interference to the scheduled user in the first cell. This method is efficiency to lead to a higher frequency reuse factor at the cell-edge, also known as 'partial frequency reuse' as demonstrated in Figure 35[9].
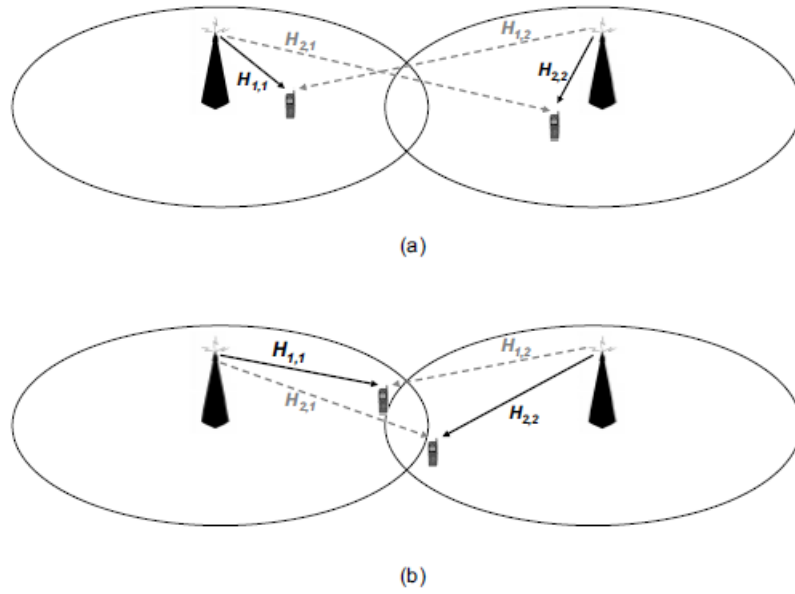
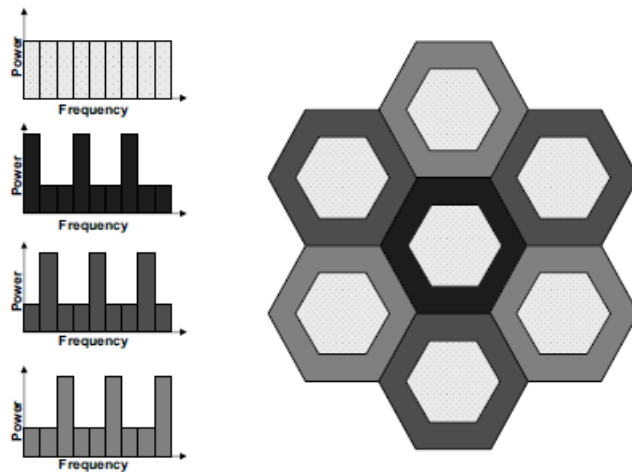**Figure 34** System configuration: (a) users close to eNBs; (b) users at the cell edge [9]

Figure 35 Partial frequency reuse [9]

CHAPTER 6

6. RESULT and ANALYSIS

6.1. THE PLANNING OF A SAMPLE TEST SYSTEM VIA ATOLL PROGRAM

6.1.1. Studying Base Stations

When we make a coverage prediction, Atoll calculates all the active and filtered base stations (i.e., that are selected by the current filter parameters) propagation zone of which intersects the rectangle containing the computation zone.

Figure 36 and 37 illustrate an example of a computation zone, in Sincan district of Ankara according to the parameters listed in Table 16. Figure 36 and Figure 37, respectively, demonstrate the signal levels of the coverage zone of eNodeB at one sector and three sectors. Here, the coverage zone expands when the sector numbers increase. On the other hand, the coverage zone is provided by making sector direction regulation sector for the zones that we want to cover while an eNodeB planning is done. In addition, the signal levels (as dBm) in the coverage zone are presented colorfully in Figure 36 and 37. On the other side, Figure 36 and Figure 37 display the signal level of the best coverage zone at -65dBm in red while -104 dBm in blue signals level shows the worst coverage zone. Figure 49 (a) and Figure 49 (b) displays the use of standard propagation model in the planning.
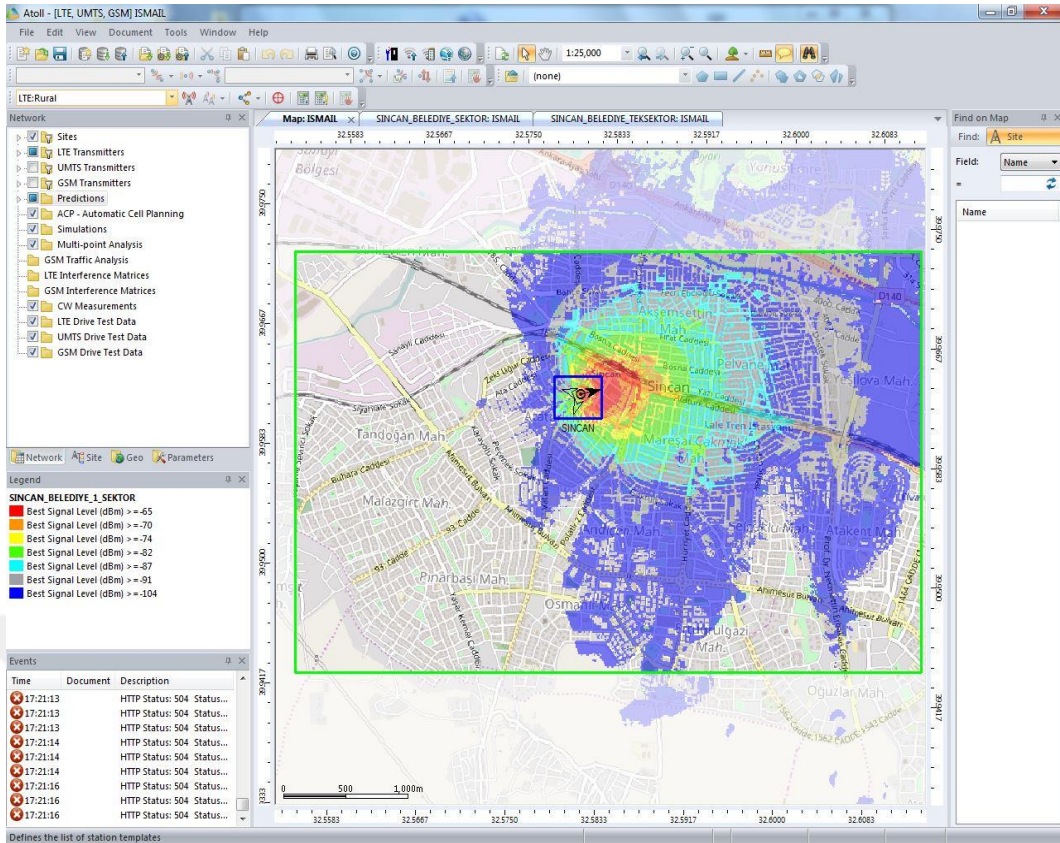
Figure 36 One Sector Coverage Zone
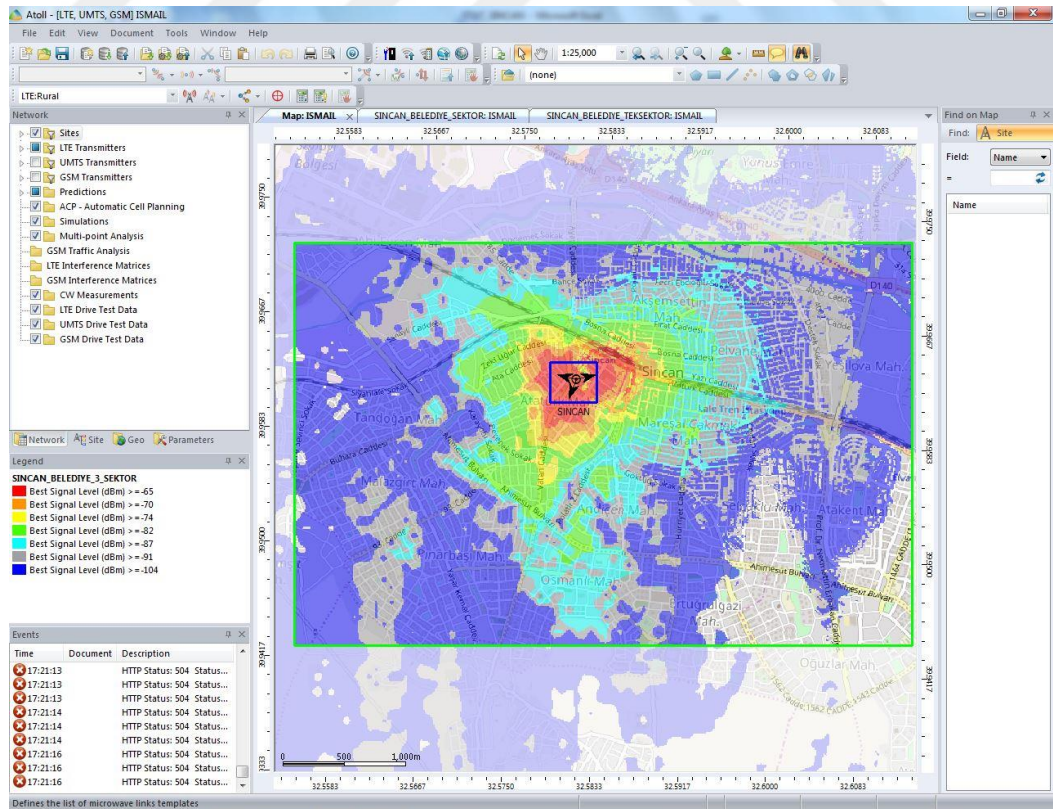
Figure 37 Three Sector Coverage Zone

The standard deviation values in the eNodeB are presented in Figure 38 and Figure 39 In addition, Figure 38 and Figure 39 also demonstrate that the coverage zone of the eNodeB, which is calculated at three sectors, is wider than the coverage zone of eNodeB calculated at one sector. Moreover, the mean and standard deviation values are observed close to each other in Figure 38 and 39. Hence, the sector number does not much affect the mean and standard deviation values. Furthermore, it just changes the propagation of the coverage zone. The coverage zone at one sector and three sectors for the eNodeB in Sincan calculate the signal levels per decibel and km^2 as presented in Table 15.
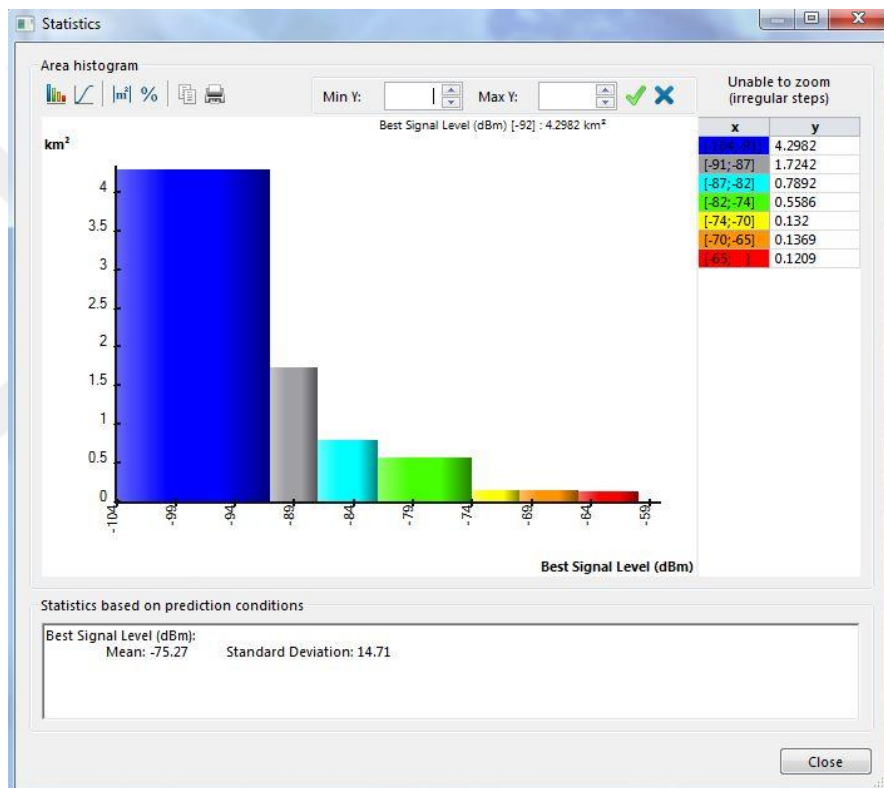
Figure 38 One Sector Standard deviations

58
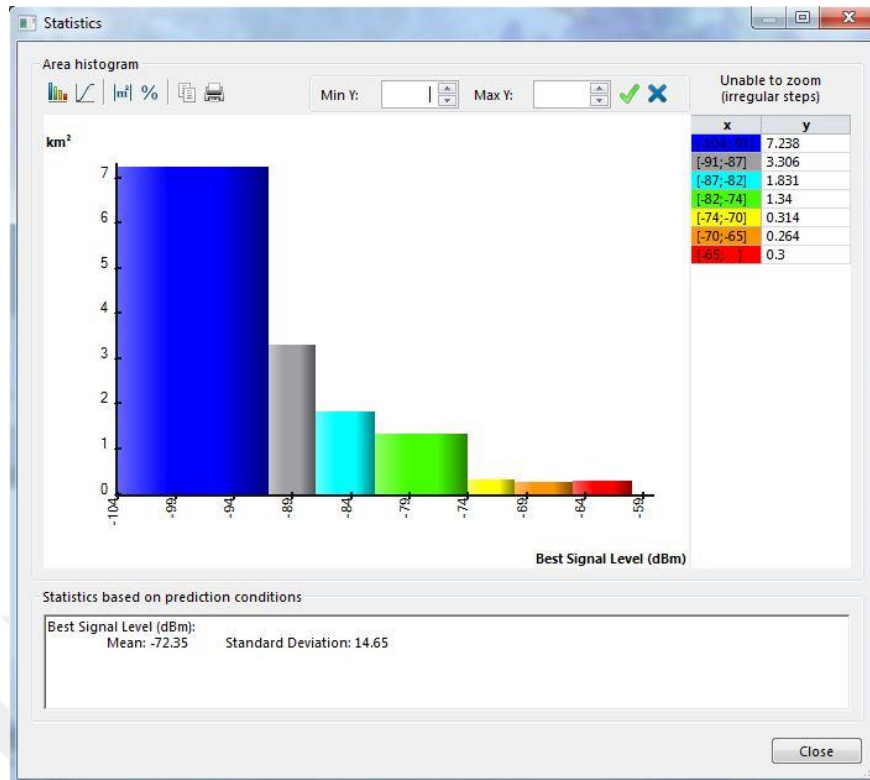
Figure 39 Three Sector Standard deviations

Prediction	Legend	Zone surface (km²)	% Focus Zone(3 SECTOR)	% Focus Zone(1 SECTOR)
SINCAN		16,3	89,7	47,7
SINCAN	Best Signal Level (dBm) >=-65	16,3	1,8	0,7
SINCAN	Best Signal Level (dBm) >=-70	16,3	3,5	1,6
SINCAN	Best Signal Level (dBm) >=-74	16,3	5,4	2,4
SINCAN	Best Signal Level (dBm) >=-82	16,3	13,6	5,8
SINCAN	Best Signal Level (dBm) >=-87	16,3	24,9	10,7
SINCAN	Best Signal Level (dBm) >=-91	16,3	45,2	21,3
SINCAN	Best Signal Level (dBm) >=-104	16,3	89,7	47,7

Table 15 Signal levels of the coverage zone of the eNodeB

Figure 40 displays the used antenna parameters. Figure 41 and Figure 42 demonstrate the propagations at horizontal and vertical of the antenna.
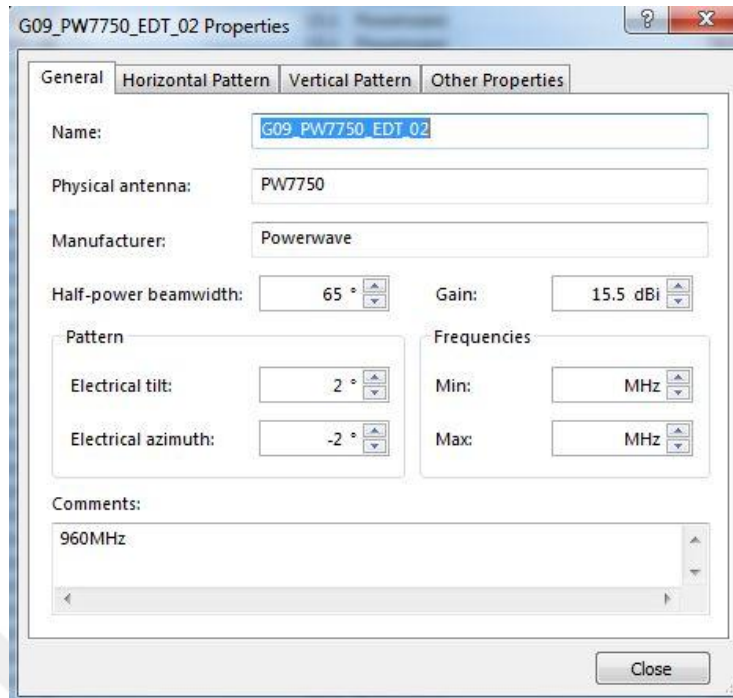
Figure 40 Used antenna parameters
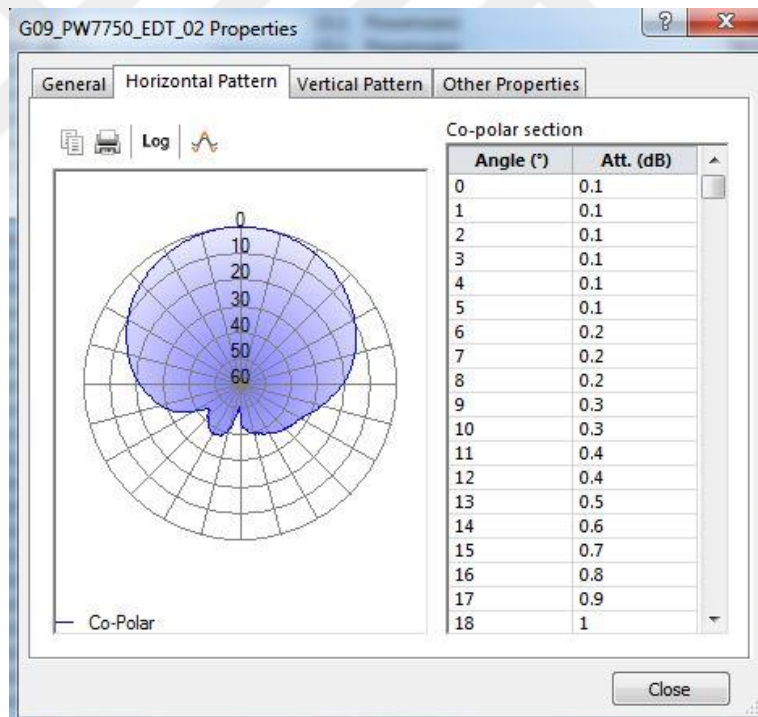
Figure 41 The propagations at horizontal of the antenna
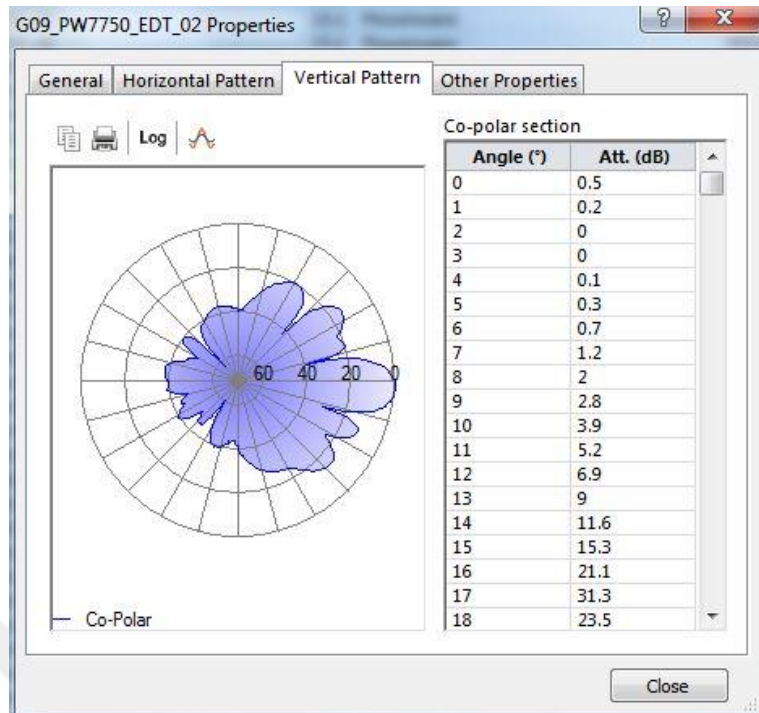
Figure 42 The propagations at vertical of the antenna
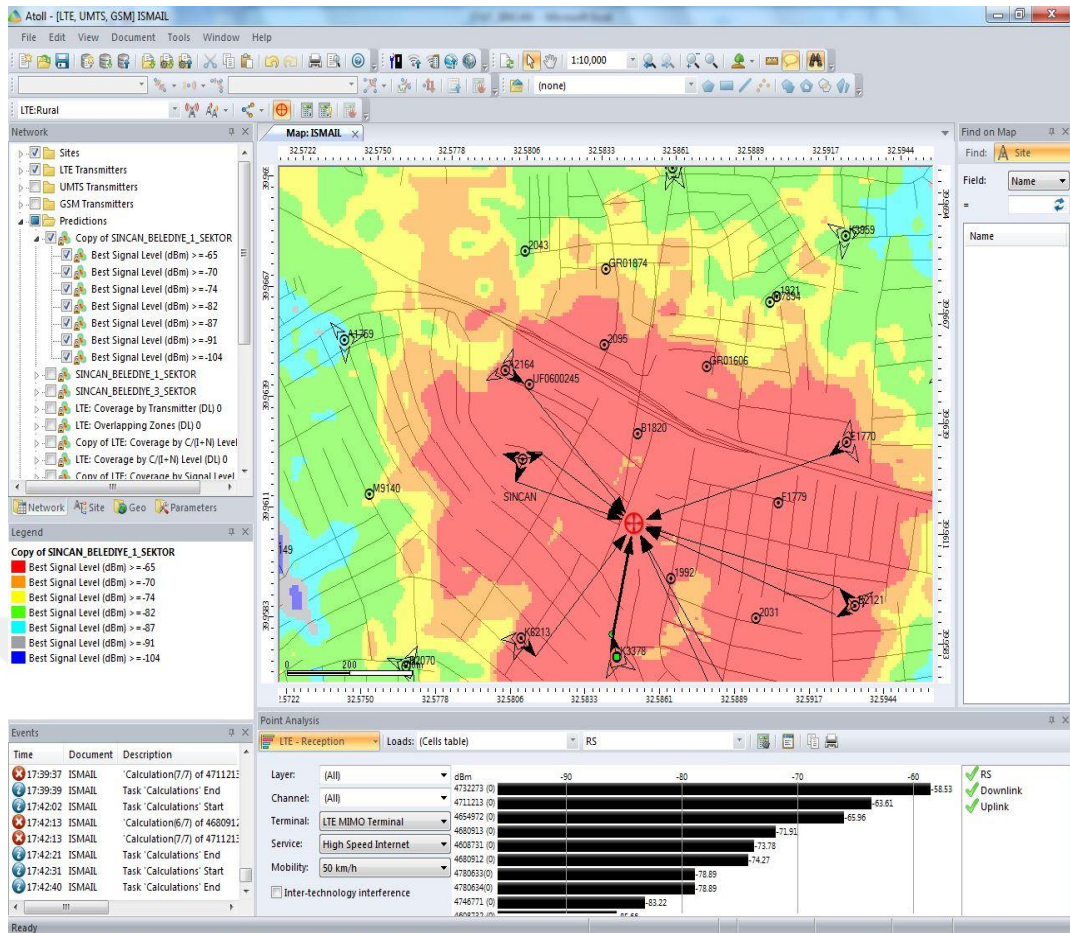
Figure 43 Panderer signal to a point

Figure 43 displays the signal levels received from the base station of the user at a sample eNodeB. The signal of this user gets service from the strongest signal level base station.

Figure 44 shows that multiple base stations s overlap with the coverage zones in the eNodeB. While coverage zone is generated, the type of antenna, antenna angle and antenna position play a crucial role to provide the same quality used at the eNodeB.
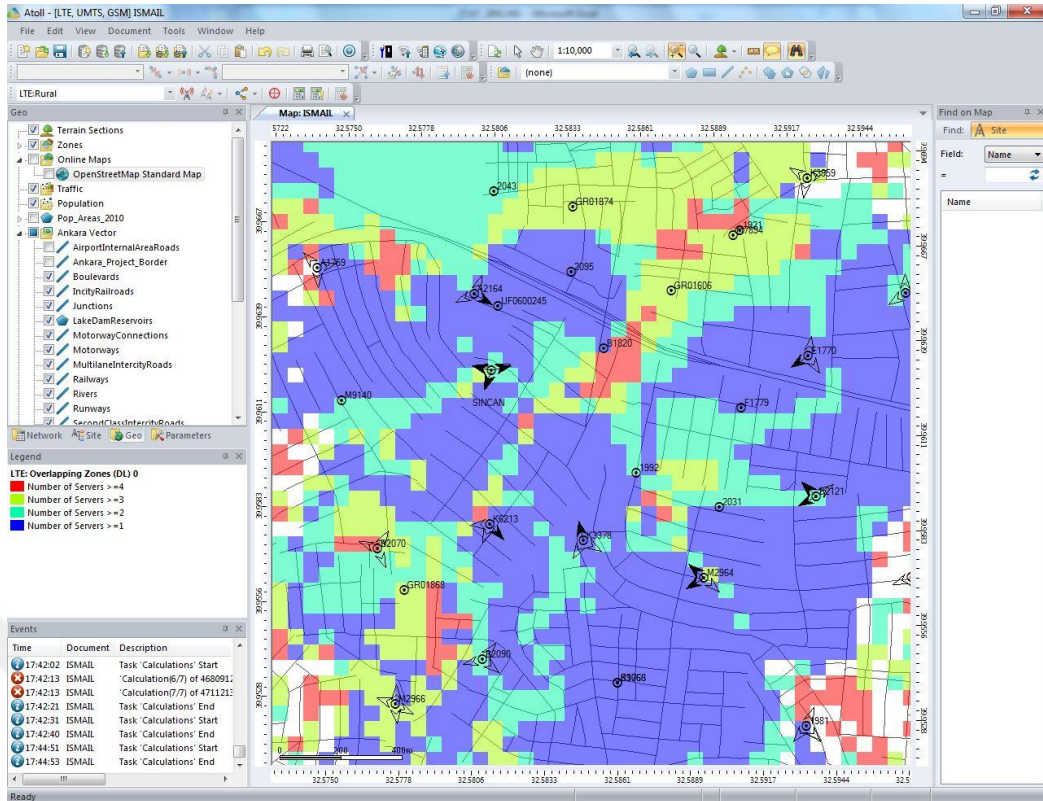
Figure 44 Overlap
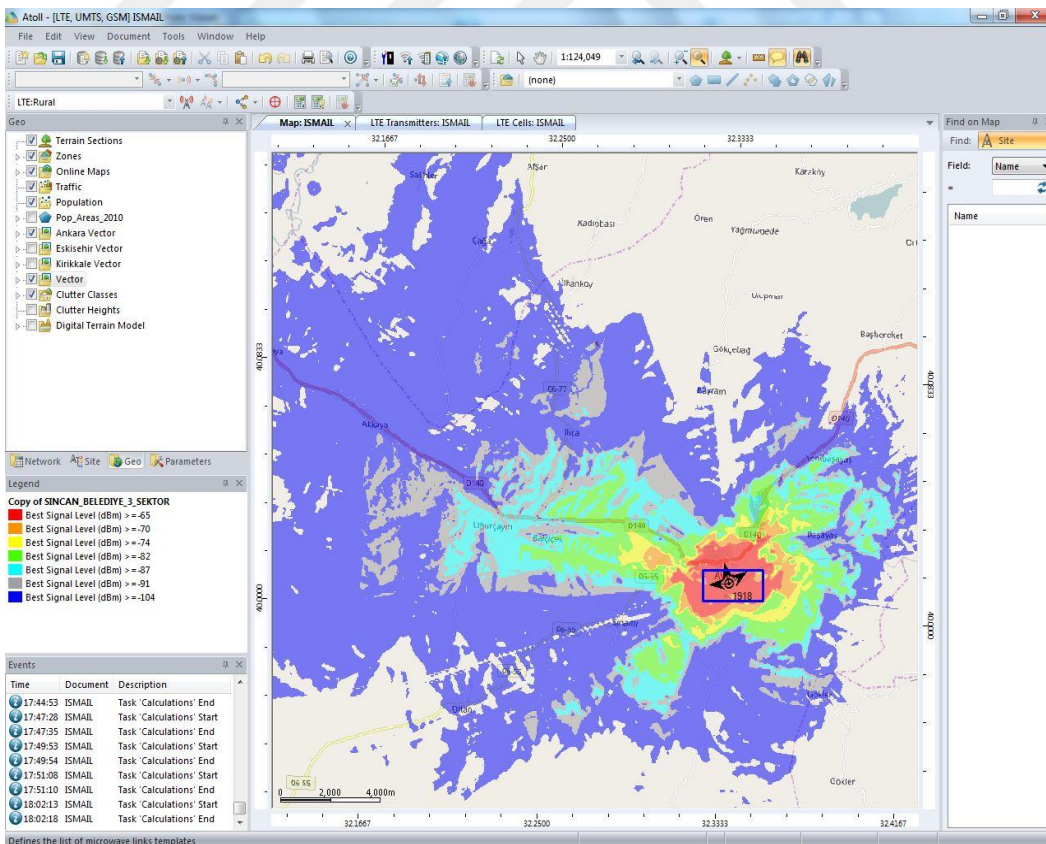
Figure 45 The coverage zone of the eNodeB at rural
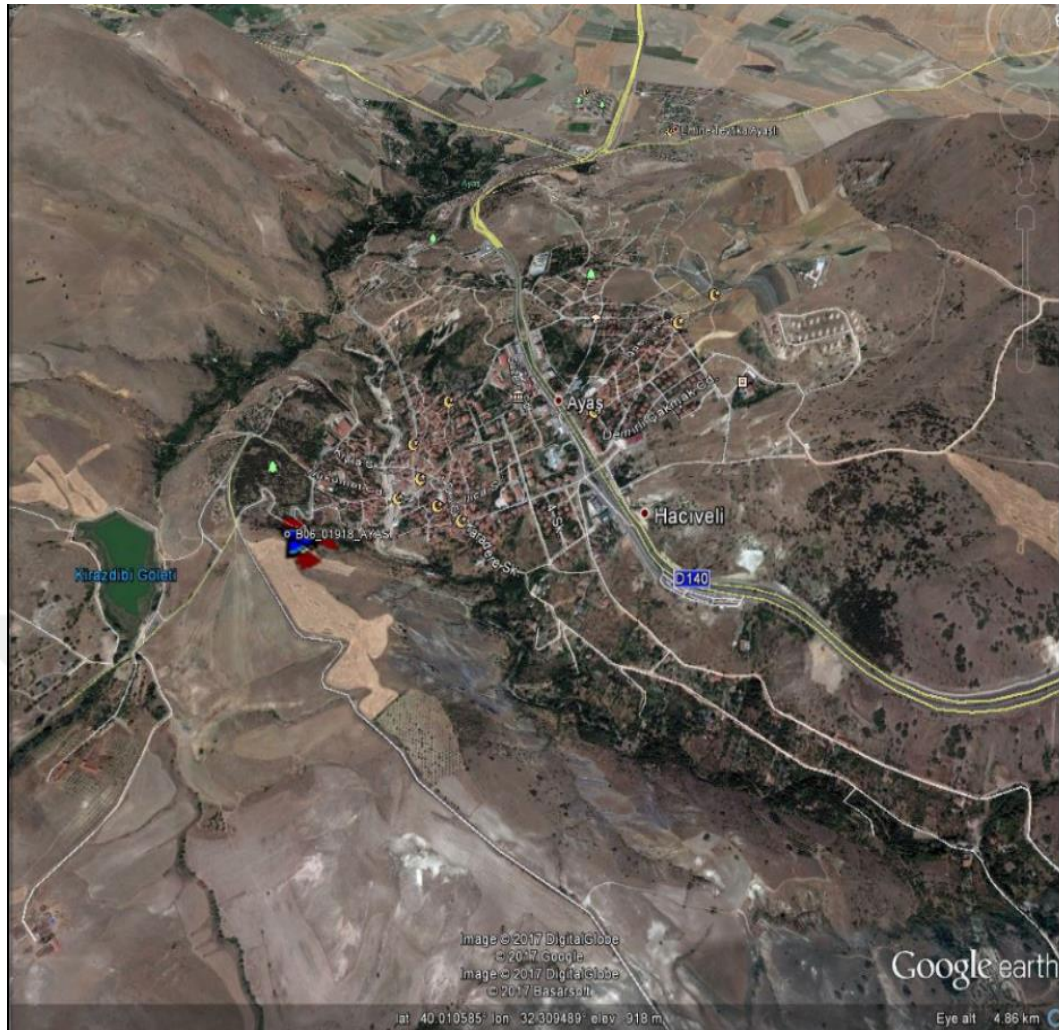
Figure 46 The geographical view of the eNodeB at rural

Figure 45 demonstrates the coverage zone of the eNodeB in rural area. Besides, the coverage zone of the base station as presented in Figure 45 and 46 displays the differences by the geographical structure.
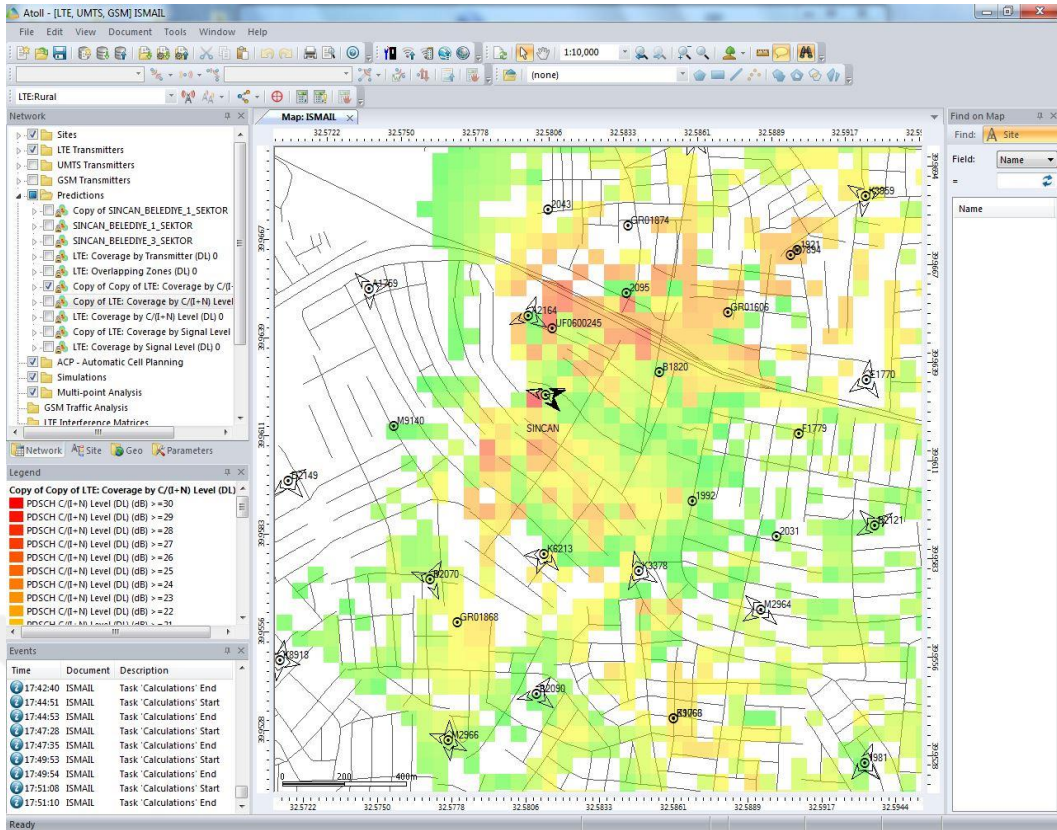
Figure 47 SINR 60°
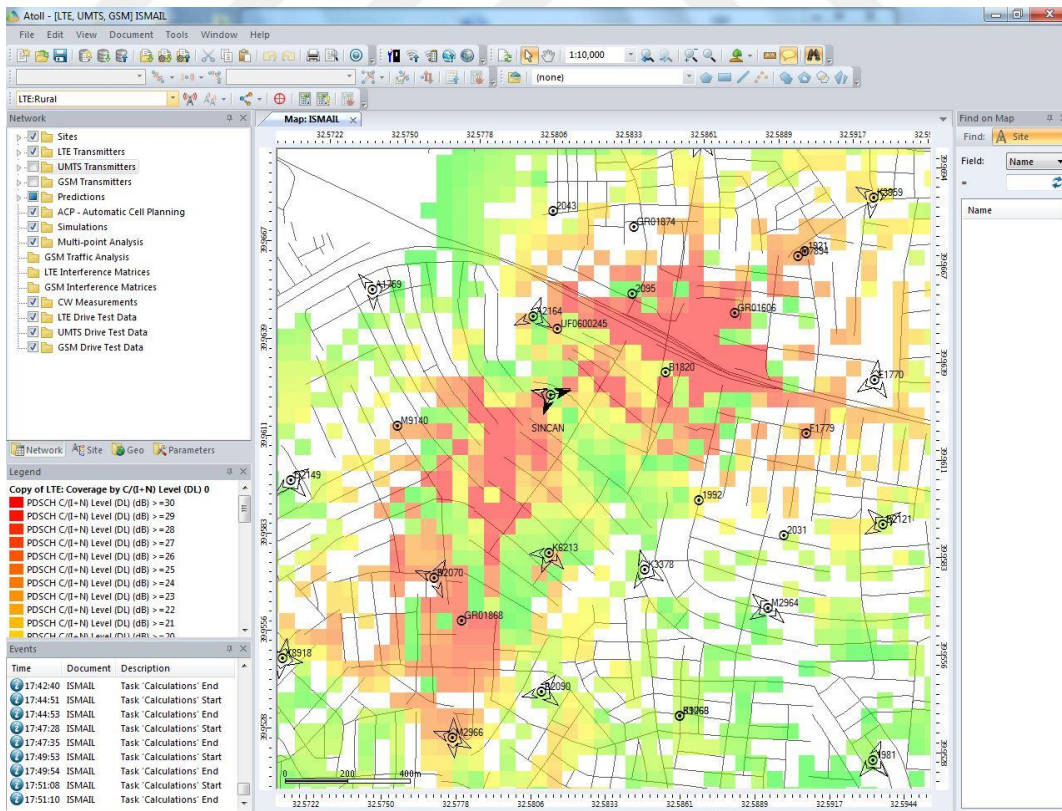
Figure 48 SINR 120°
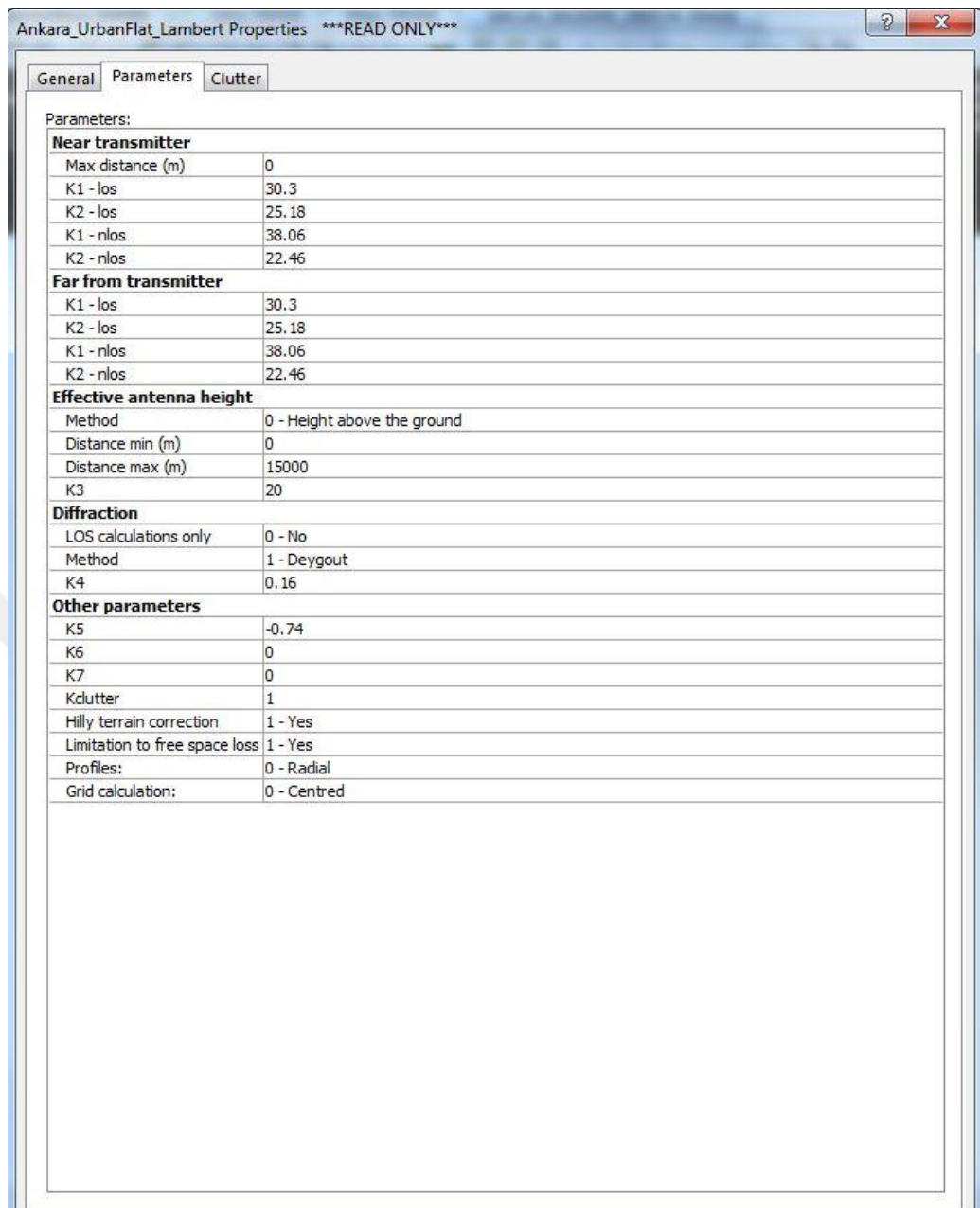
Figure 49 (a) Use of the standard propagation model in the planning
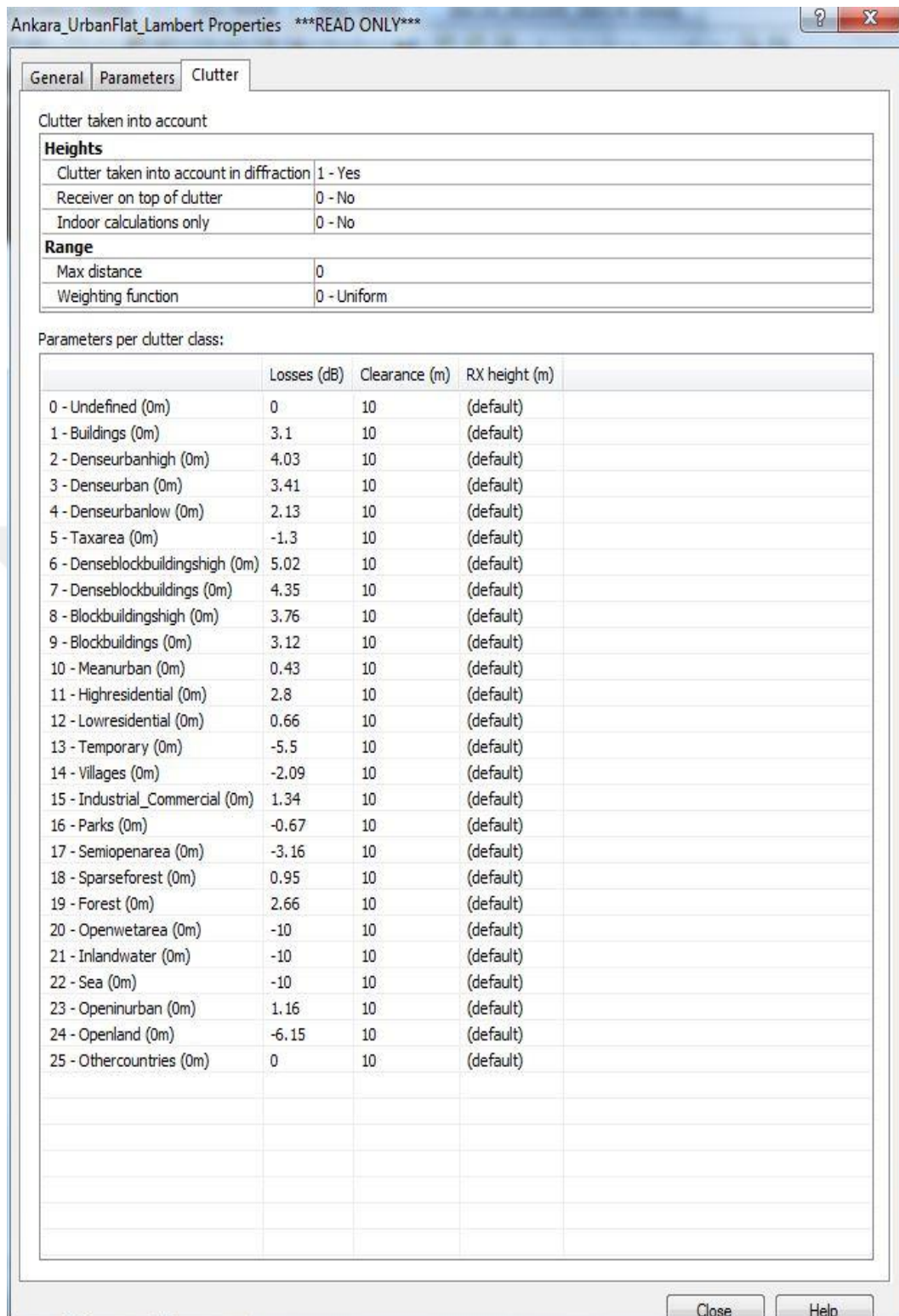
Figure 49 (b) Use of the standard propagation model in the planning

Figure 47 and 48 change the coverage zone through angle modifications between sectors. For instance, Figure 47 and 48 demonstrate the coverage zone

changes when $60°$ and $120°$ are used between sectors. The SNR problem results from increasing interference while the angle between sectors is decreased. The effect of the data rate values on the user decreases.

In this section, the analysis of the capacity and coverage will be calculated by using current parameters of the LTE network which is still under test conditions in Turkey as presented in Figure 37.

	Parameters	Values
a	Carrier frequency	900 MHz
b	Bandwidth	10 MHz
c	Number of Sector	3 Sector
d	MIMO	1x1
e	Antenna Gain of Receiver (eNode B) Base Station(G_{TX})	20 dBi
f	Output Power of Base Station(TX_{PWR})	46 dBm
g	Cable loss of Transmitter Base Station(eNode B)	2
h	Noise Figure of Base Station (F)	4 dB
i	Micro cell base station's height(Dhb)	25 m
j	Antenna height of User Equipment(Hm)	1.5m
k	UE Noise Figure(dB)	9dB
l	Thermal Noise Density(dBm) for Receiver(UE)	-104.5 dBm
m	UE(Receiver) Antenna Gain(dBi)	0
n	eNode B(Reveiver) Thermal Noise Density(dBm)	-118.4 dBm
p	Control Channel Headings (%) for Receiver- UE	20
r	SINR(dB) for Receiver -UE	-9
s	Interference Tolerance(dBm) for Receiver- UE	4
t	Body loss(dB) for Receiver- UE	0
u	Max. Transmitter- UE Power (dBm)	23
w	Transmitter-UE antenna gain(dBi)	0
x	Receiver-eNode B Noise Figure(dB)	5
v	SINR(dB) for Receiver - eNode B	-7
y	Interference Tolerance(dBm) for Receiver- eNode B	3
z	Cable Loss(dB) for Receiver- eNode B	0
o	Fast Fading Tolerance (dB) for Receiver-eNode B	0

Table 16 Working Parameters of Test Network

According to the data presented in Table 16, the equations (5.7) and (5.8) calculated the downlink and uplink as presented in Figure 50 from the calculated band efficiency and SNR efficiency values in Table 10.
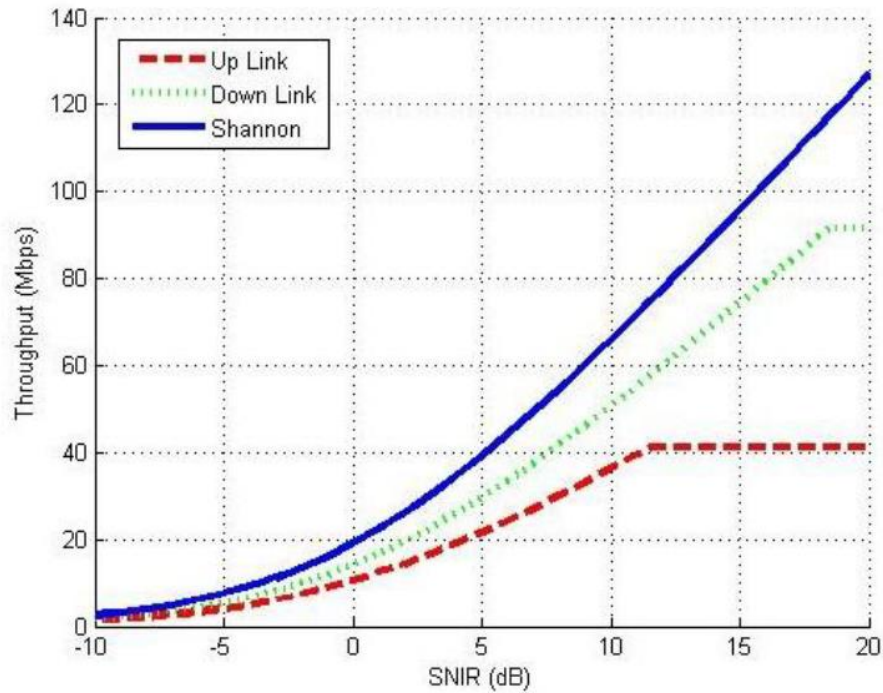
Figure 50 Downlink and Uplink Capacity

In section 5.3, all control channel headings were calculated and link level bandwidth efficiency was found around 0.8. The coverage area of control channel headings is 20 %. The attenuation value which is eventuated by the control channel headings in this ratio is between 0.2-1 dB. In this calculation, this value was taken as 1 dB.

Downlink calculation of the network for Maximum Path Loss (PL):

In data rate calculations, the downlink was taken 1024 kbps. According to this, SINR value is observed in -9dB as presented in Figure 50.

EIRP (dBm) =**f**+**e**-**g**= 46+20-2= 64 dBm

Receiver Noise Power (dBm) =**k**+**l**=9-104.5= -95.5 dBm

Receiver Sensitivity (dBm)= Receiver Noise Power(dBm) + **r** = -95.5-9= -104.5 dBm

Maximum Path Loss (PL) = EIRP (dBm)- Receiver Sensitivity (dBm)-**s**-**p**-**t**+**m**= 64+104.5-4-1-0+0=**163.5 dBm**

Uplink calculation of the network for Maximum Path Loss (PL):

In data rate calculations, the downlink was taken 64 kbps. Accordingly, SINR value is observed in -7dB as presented in Figure 50.

EIRP (dBm) =**u**+**w**= 23dBm

Receiver Noise Power (dBm)=**x** + **n**= 5-118.4 =-116.4 dBm

Receiver Sensitivity (dBm)= Receiver Noise Power (dBm)+ **v** = -116.4-7=-123.4dBm

Maximum Path Loss (PL) = EIRP (dBm)- Receiver Sensitivity (dBm)-**y**-**z**+**e**-**o**=23+123.4-3-0+20-0=**163.4 dBm**

The result of the maximum path loss in downlink calculations was observed as 163.5 dB. Section 5 shows that we could not obtain the correct result since using frequency for the path loss statement is not exactly between 800-2000MHz. Cell radius with path loss computing application in online reference [1] for found loss was detected as nearly 1200m. Similarly, when cell radius for uplink was calculated, it was found 1100m.

According to test results of the network, instant total capacity of the base station becomes 60 users when we assume that all users are using mobile equipments which has same features with category 2 listed in Table 12 to the data rate based dimensioning for the average 50 Mbps downlink data speed.
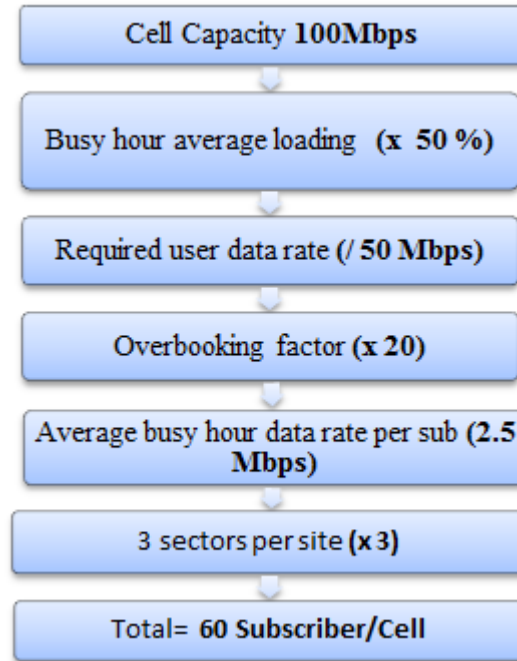
Figure 51 Data Rate based dimensioning of Test Network

6.1.2. LTE Planning in the province of Çankırı

In order to conduct an LTE planning study, Atoll Tool is needed for the geographical map as well as the population map of the region where the planning will be conducted. To illustrate, the following map demonstrates how LTE planning is carried out in the province of Çankırı. Figure 52 displays black dots presenting where the human population is located within the province borders of Çankırı. Figure 53 displays the yellow dots presenting human population and the land forms (clutter vectors) in the province of Çankırı.

71
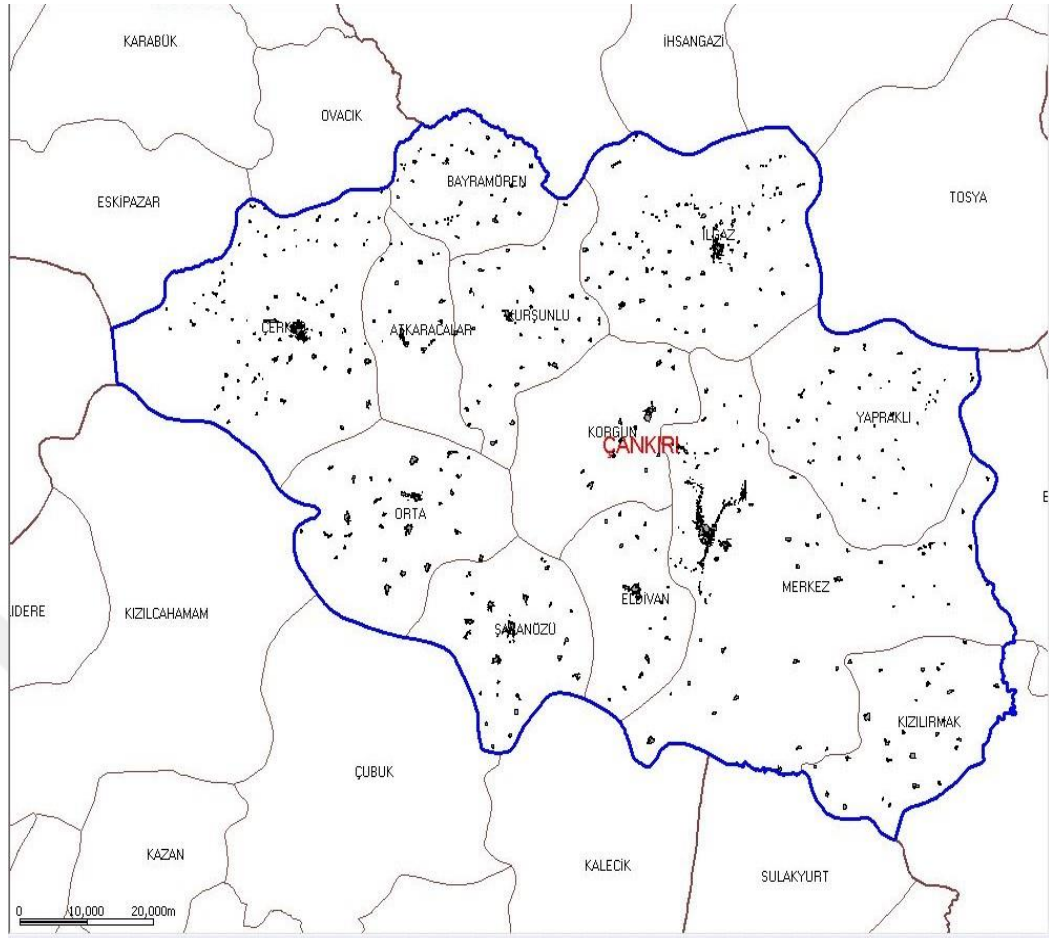
Figure 52 Population distribution within the borders of Çankırı province
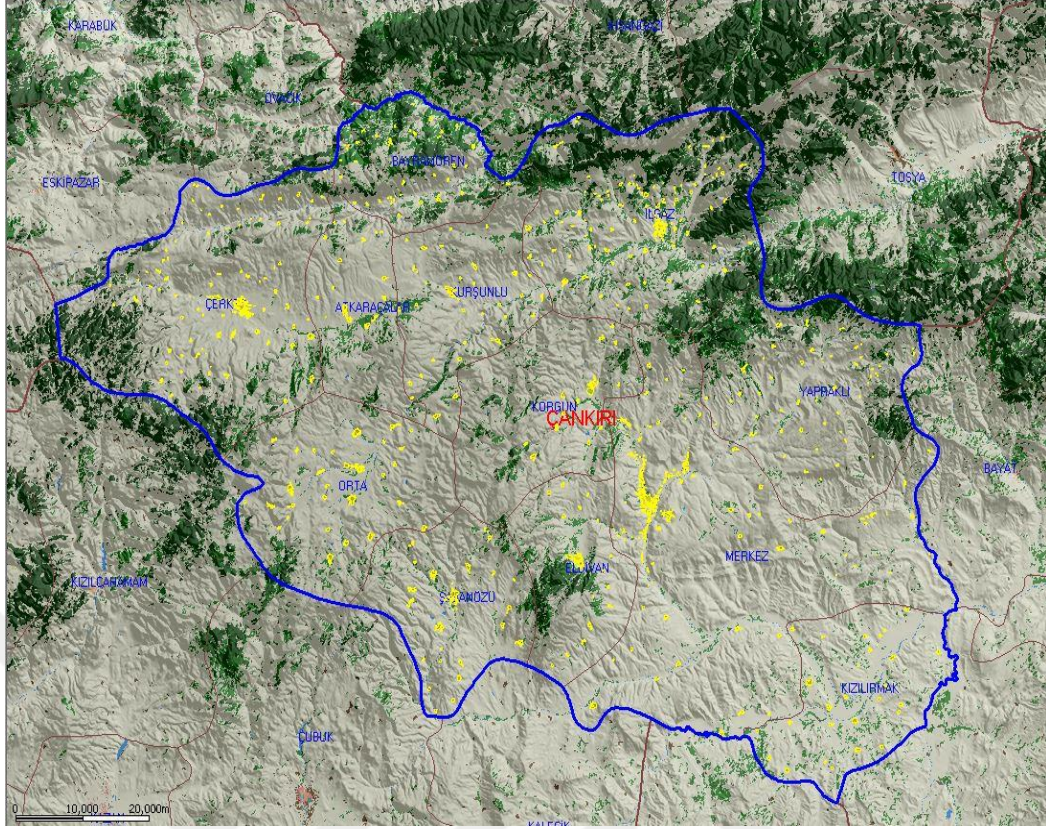
Figure 53 The human population and the land forms (clutter vectors) distribution of
Çankırı province

When the first planning of the region is conducted, the LTE planning is
carried out in accordance with the standard propagation model (Figure 57 (a) and
Figure 57 (b)) which is included in the Atoll Tool. In this study, the coverage area
includes population-dense areas, being the province, the town, the grand villages
involving more than 1500 population in the center. When Radio Frequency (RF)
antenna heights are taken up to approximately 18 meters at height for the city center
and 40 meters for the other coverage areas in the first LTE planning of Çankırı
province, the coverage map can be displayed as presented in Figure 54. In addition, it
is adjusted with the $0° − 120° − 240°$ angle between the sectors. The statistical
results generated from these adjustments are displayed in Table 17. 62, 1 km^2 in
Table 17 is indicated as the coverage area of the total population of Çankırı province
(the surface area of Çankırı province is 7558 km^2). The coverage area of some of
the base stations does not seem alike as presented in Figures 54, 55 and 56 since
these base stations take solely 2G service (such as Site_44, Site_45, Site_50,Site_70
etc.).

Figure 54 The coverage area in the first planning of Çankırı province via Atoll Tool

Zone	Legend	Zone surface (km²)	% Focus Zone	Surface (km²)	% of Covered Area
Focus Zone		62.1	14.7	9.104	100
Focus Zone	Best Signal Level (dBm) >=-70	62.1	0.3	0.173	1.9
Focus Zone	Best Signal Level (dBm) >=-75	62.1	0.6	0.392	4.306
Focus Zone	Best Signal Level (dBm) >=-80	62.1	1.2	0.774	8.502
Focus Zone	Best Signal Level (dBm) >=-85	62.1	2.2	1.364	14.982
Focus Zone	Best Signal Level (dBm) >=-90	62.1	3.4	2.095	23.012
Focus Zone	Best Signal Level (dBm) >=-95	62.1	5.2	3.254	35.743
Focus Zone	Best Signal Level (dBm) >=-100	62.1	9.2	5.738	63.027
Focus Zone	Best Signal Level (dBm) >=-105	62.1	14.7	9.104	100

Table 17 The statistical results of the first planning of Çankırı province

In the second planning of Çankırı province, the antenna heights are adjusted according to the location of the site to be planned and the antenna directions are adjusted according to the coverage area. At the end of these adjustments, the coverage area map is obtained and presented in Figure 55. The statistical results generated from these adjustments are displayed in Table 18.
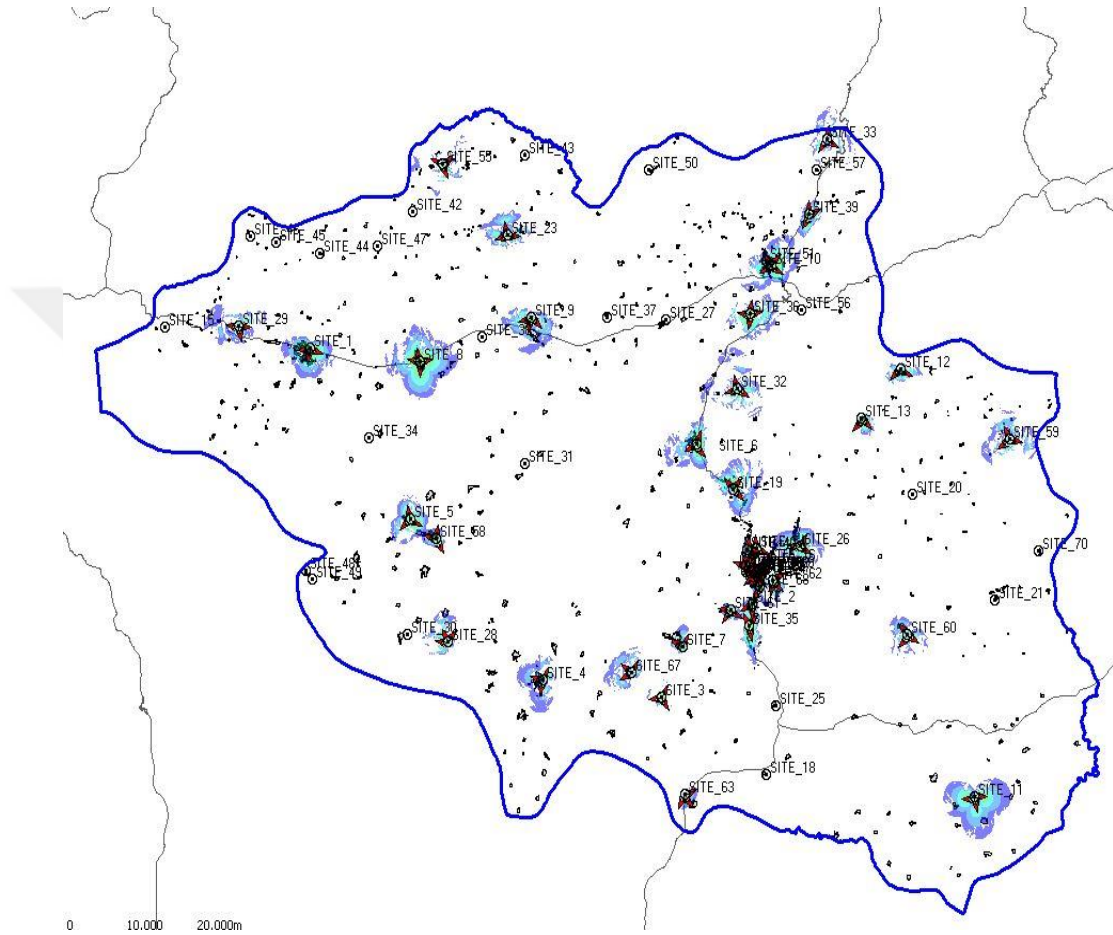
Figure 55 The coverage area in the second planning of Çankırı province via Atoll Tool

Zone	Legend	Zone surface (km²)	% Focus Zone	Surface (km²)	% of Covered Area
Focus Zone		62.1	20.9	12.96	100
Focus Zone	Best Signal Level (dBm) >=-70	62.1	0.3	0.166	1.281
Focus Zone	Best Signal Level (dBm) >=-75	62.1	0.6	0.389	3.002
Focus Zone	Best Signal Level (dBm) >=-80	62.1	1.3	0.788	6.08
Focus Zone	Best Signal Level (dBm) >=-85	62.1	2.4	1.519	11.721
Focus Zone	Best Signal Level (dBm) >=-90	62.1	4.5	2.786	21.497
Focus Zone	Best Signal Level (dBm) >=-95	62.1	7.8	4.864	37.531
Focus Zone	Best Signal Level (dBm) >=-100	62.1	13.5	8.359	64.498
Focus Zone	Best Signal Level (dBm) >=-105	62.1	20.9	12.96	100

Table 18 The statistical results of the second planning of Çankırı province

Comparing Table 17 and Table 18, we can see the values of -105 dBm; the coverage area in the first planning is 14.7% while it is 20.9% in the second planning.

When the third planning is conducted via another standard propagation model (Figure 58 (a) and Figure 58 (b)) than the model in the first planning and second planning, the coverage area map obtained is presented in the following Figure 56. The statistical results generated from these adjustments were displayed in Table 19.
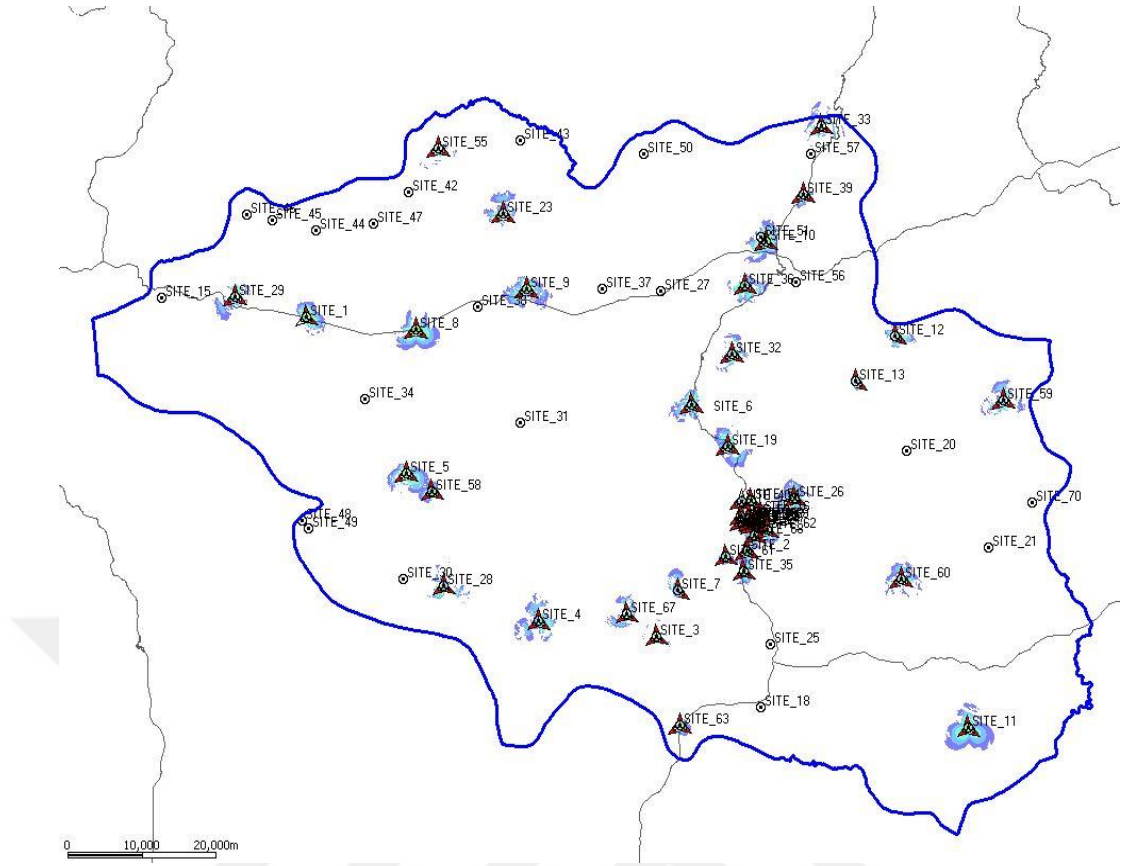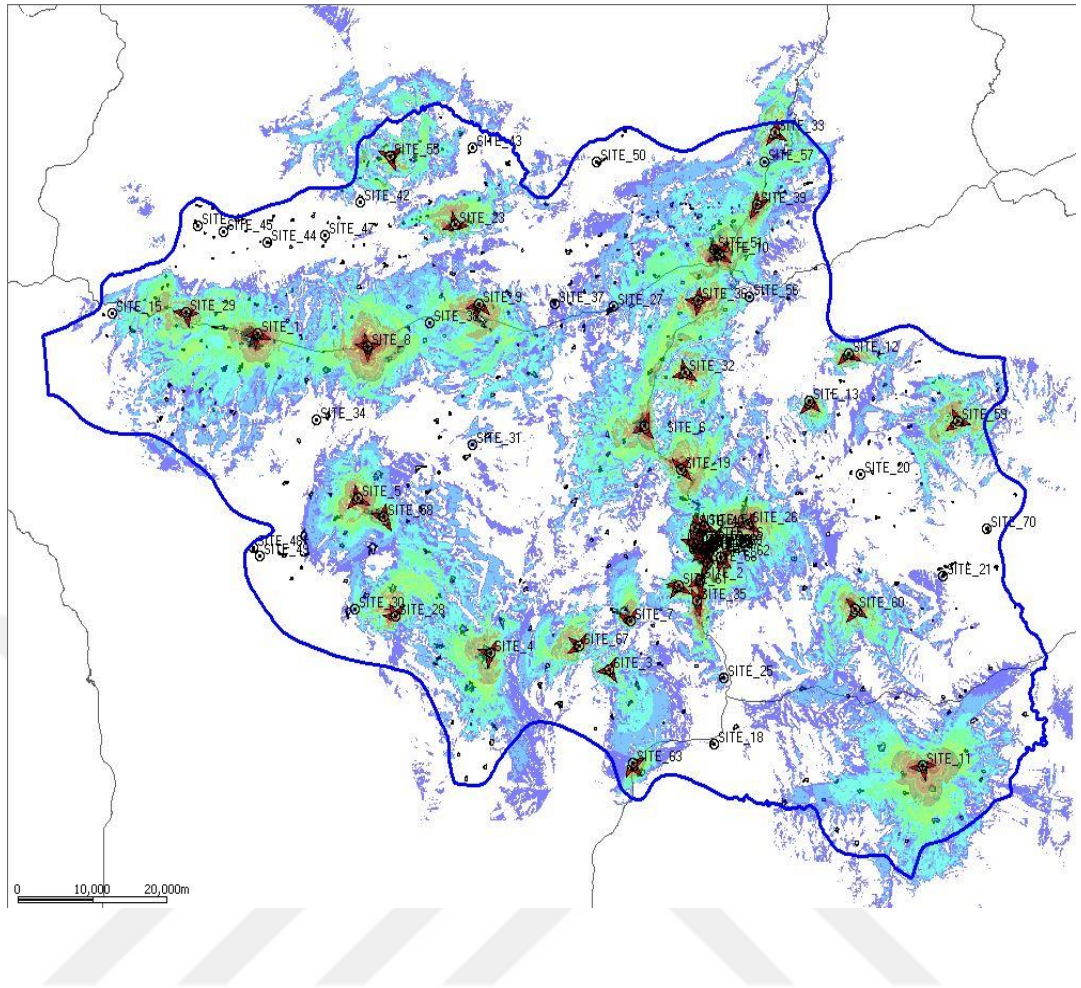
Figure 56 The coverage area in the third planning of Çankırı province via Atoll Tool

Zone	Legend	Zone surface (km²)	% Focus Zone	Surface (km²)	% of Covered Area
Focus Zone		62.1	66.6	41.386	100
Focus Zone	Best Signal Level (dBm) >=-70	62.1	4.7	2.902	7.012
Focus Zone	Best Signal Level (dBm) >=-75	62.1	7.8	4.871	11.77
Focus Zone	Best Signal Level (dBm) >=-80	62.1	13.8	8.593	20.763
Focus Zone	Best Signal Level (dBm) >=-85	62.1	20.6	12.798	30.924
Focus Zone	Best Signal Level (dBm) >=-90	62.1	29.9	18.594	44.928
Focus Zone	Best Signal Level (dBm) >=-95	62.1	40.7	25.25	61.011
Focus Zone	Best Signal Level (dBm) >=-100	62.1	53.5	33.228	80.288
Focus Zone	Best Signal Level (dBm) >=-105	62.1	66.6	41.386	100

Table 19 The statistical results of the third planning of Çankırı province

Comparing Table 17, Table 18 and Table 19, we can see the values of -105 dBm; the coverage area in the first planning is 14.7% while it is 66.6% in the third planning. The model parameters to be used in the planning determine the result of the real measurement obtained from field. Furthermore, the optimum value is obtained according to this result.

In conclusion, the antenna heights, the angles between the sectors and the standard propagation model of the base stations are altered to determine the best coverage area map of the region to be planned. The investments of the region are conducted according to the highest coverage area.

Parameters:

Near transmitter	
Max distance (m)	0
K1 - los	17.4
K2 - los	44.9
K1 - nlos	17.4
K2 - nlos	44.9
Far from transmitter	
K1 - los	17.4
K2 - los	44.9
K1 - nlos	17.4
K2 - nlos	44.9
Effective antenna height	
Method	0 - Height above the ground
Distance min (m)	0
Distance max (m)	15000
K3	5.83
Diffraction	
LOS calculations only	0 - No
Method	1 - Deygout
K4	1
Other parameters	
K5	-6.55
K6	0
K7	0
Kclutter	0
Hilly terrain correction	0 - No
Limitation to free space loss	1 - Yes
Profiles:	0 - Radial
Grid calculation:	0 - Centred

Figure 57 (a) Use of the Standard propagation model in the first and second planning

Clutter taken into account

Heights	
Clutter taken into account in diffraction	1 - Yes
Receiver on top of clutter	0 - No
Indoor calculations only	0 - No
Range	
Max distance	0
Weighting function	0 - Uniform

Parameters per clutter class:

	Losses (dB)	Clearance (m)	RX height (m)
0 - Undefined (0m)	0	10	(default)
1 - Buildings (0m)	0	10	(default)
2 - Denseurbanhigh (0m)	0	10	(default)
3 - Denseurban (0m)	0	10	(default)
4 - Denseurbanlow (0m)	0	10	(default)
5 - Taxarea (0m)	0	10	(default)
6 - Denseblockbuildingshigh (0m)	0	10	(default)
7 - Denseblockbuildings (0m)	0	10	(default)
8 - Blockbuildingshigh (0m)	0	10	(default)
9 - Blockbuildings (0m)	0	10	(default)
10 - Meanurban (0m)	0	10	(default)
11 - Highresidential (0m)	0	10	(default)
12 - Lowresidential (0m)	0	10	(default)
13 - Temporary (0m)	0	10	(default)
14 - Villages (0m)	0	10	(default)
15 - Industrial_Commercial (0m)	0	10	(default)
16 - Parks (0m)	0	10	(default)
17 - Semiopenarea (0m)	0	10	(default)
18 - Sparseforest (0m)	0	10	(default)
19 - Forest (0m)	0	10	(default)
20 - Openwetarea (0m)	0	10	(default)
21 - Inlandwater (0m)	0	10	(default)
22 - Sea (0m)	0	10	(default)
23 - Openinurban (0m)	0	10	(default)
24 - Openland (0m)	0	10	(default)
25 - Othercountries (0m)	0	10	(default)

Figure 57 (b) Use of the Standard propagation model in the first and second planning

Parameters:

Near transmitter	
Max distance (m)	0
K1 - los	48
K2 - los	30.15
K1 - nlos	67.92
K2 - nlos	24.02
Far from transmitter	
K1 - los	48
K2 - los	30.15
K1 - nlos	67.92
K2 - nlos	24.02
Effective antenna height	
Method	0 - Height above the ground
Distance min (m)	0
Distance max (m)	15000
K3	-13.84
Diffraction	
LOS calculations only	0 - No
Method	3 - Deygout with correction (ITU526-5)
K4	0.39
Other parameters	
K5	0
K6	0
K7	0
Kclutter	1
Hilly terrain correction	0 - No
Limitation to free space loss	1 - Yes
Profiles:	0 - Radial
Grid calculation:	0 - Centred

Figure 58 (a) Use of the Standard propagation model in the third planning

Clutter taken into account

Heights	
Clutter taken into account in diffraction	0 - No
Receiver on top of clutter	0 - No
Indoor calculations only	0 - No
Range	
Max distance	0
Weighting function	0 - Uniform

Parameters per clutter class:

	Losses (dB)	Clearance (m)	RX height (m)
0 - Undefined (0m)	0	10	(default)
1 - Buildings (0m)	-1.62	10	(default)
2 - Denseurbanhigh (0m)	2.41	10	(default)
3 - Denseurban (0m)	2.41	10	(default)
4 - Denseurbanlow (0m)	2.41	10	(default)
5 - Taxarea (0m)	-5.96	10	(default)
6 - Denseblockbuildingshigh (0m)	2.41	10	(default)
7 - Denseblockbuildings (0m)	2.41	10	(default)
8 - Blockbuildingshigh (0m)	-1.62	10	(default)
9 - Blockbuildings (0m)	-1.62	10	(default)
10 - Meanurban (0m)	-4.03	10	(default)
11 - Highresidential (0m)	-1.57	10	(default)
12 - Lowresidential (0m)	-1.57	10	(default)
13 - Temporary (0m)	-1.57	10	(default)
14 - Villages (0m)	-7.92	10	(default)
15 - Industrial_Commercial (0m)	-1.83	10	(default)
16 - Parks (0m)	-3.26	10	(default)
17 - Semiopenarea (0m)	-5.96	10	(default)
18 - Sparseforest (0m)	-4.3	10	(default)
19 - Forest (0m)	-7.01	10	(default)
20 - Openwetarea (0m)	-12	10	(default)
21 - Inlandwater (0m)	-13	10	(default)
22 - Sea (0m)	-14	10	(default)
23 - Openinurban (0m)	-3.26	10	(default)
24 - Openland (0m)	-9.11	10	(default)
25 - Othercountries (0m)	0	10	(default)

Figure 58 (b) Use of the Standard propagation model in the third planning

CHAPTER 8

7. CONCLUSION

Although the planning was made manually in the past, 4.5G network planning processes are made for the planning via the special program tools (RF optimization tools like Atoll, OSS, TEMS, Actix, Mapinfo, Mentor-Forte, and Nastar) in our day. A base station working with taking program tools Google Maps is planned in consideration of the geographical conditions. On the other hand, the coverage knowledge of the customers at the site along with LTE is followed up. At the end of the follow-up process, necessary planning is conducted.

REFERENCES

[1] **GSA (2017),** "*GSA: Evolution to LTE Report- January 2017*", https://gsacom.com/paper/gsa-evolution-lte-report-january-2017/.

[2] **Tondare S. M., Panchal S. D. , Kushnure D. T. (2014),** "*Evolutionary steps from 1G to 4.5 G.*", International Journal of Advanced Research in Computer and Communication Engineering 3, no. 4, pp. 6163-6166.

[3] **Berardinelli G., Frattasi S., et. al. (2008),** "*OFDMA vs. SC-FDMA: Performance comparison in local area IMT-A Scenarios*", IEEE Wireless Communications, pp. 64-72.

[4] **Vieira P., Queluz P., Rodrigues A. (2008),** "*MIMO antenna array impact on channel capacity for a realistic macro-cellular urban environment*", 68th IEEE Vehicular Technology Conference Fall 2008 Calgary, Canada, September, pp. 1-5.

[5] **Cui D. (2009),** "*LTE peak rates analysis*", Wireless and Optical Communications Conference, pp. 1-3.

[6] **Kavas A., (2003),** "*Cellular Mobile Radio System Design Using Path Loss Calculations*", 3rd International Conference on Electrical and Electronics Engineering, Bursa-Turkey, pp-290-293, Vol.Electronic ISBN: 975-395-667-3.

[7] **Huawei Technologies Co., Ltd (2010),** "*LTE Air Interface Training Manual*", pp. 1-2.

[8] **Zarrinkoub H., (2014),** "*Understanding LTE with MATLAB from Mathematical Modeling to Simulation and Prototyping*", John Wiley& Sons, pp. 2-4.

[9] **Sesia S., Toufik I., Baker M., (2009)** "*LTE, the UMTS Long Term Evolution from Theory to Practice*", John Wiley & Sons, pp.7-8, 141-144, 208-209, 294-297, 422-423, 521-522.

[10] **Holma H. and Toskala A. (2009),** "*LTE for UMTS – OFDMA and SC-FDMA Based Radio Access*", John Wiley & Sons, pp.8-9, 25-30, 216, 247-248.

[11] **3gwiz (2015),** "*Optus Demonstrates 480 Gbps on LTE-CA*",

http://3gwiz.com.au/ozmobilenet/?m=201503, March.

[12] Gesssner C., Roessler A., Kotttkamp M. (2010), "*UMTS Long Term Evolution (LTE) Technologies Introduction*", Rohde& Schwarz, May, pp. 10.

[13] AhmadZadeh A. M. (2008), "*Capacity and Cell-Range Estimation for Multitraffic Users in Mobile WiMax*", University college of Borås Sweden, pp. 7.

[14] Rumney M (2010), "*3GPP LTE: Introducing Single-Carrier FDMA*",
http://cp.literature.agilent.com/litweb/pdf/5989-7898EN.pdf, May, pp. 5-6.

[15] 3GPP TS 36.213(2013), "*Evolved Universal Terrestrial Radio Access (E-UTRA); Physical layer procedures*", Version 11.2.0 Release 11, April, pp.69, 82.

[16] Ericsson (2010), "*LTE – an introduction*",
http://squiz.informatm.com/__data/assets/pdf_file/0006/190527/lte_overview_Ericsson.pdf, May, pp.6-7.

[17] 3GPP TS 36.101(2012), "*Evolved Universal Terrestrial Radio Access (E-UTRA); User Equipment (UE) radio transmission and reception*", Version 10.6.0 Release 10, March, pp.21.

[18] 3GPP TS 36.211(2014), "*Evolved Universal Terrestrial Radio Access (E-UTRA); Physical Channels and Modulation*", Version 11.6.0 Release 11, October, pp.57, 89.

[19] Ekström H., Furuskär A., Karlsson J., Meyer M., Parkvall S., Torsner J., Wahlqvist M. (2006), "*Technical Solution for the 3G Long-Term Evolution*", IEEE Communications Magazine, March, pp.42.

[20] Dahlman E., Parkvall S., Skold J., Beming P. (2008), "*3G evolution: HSPA and LTE for mobile Broadband*", Second edition, Elsevier Academic Press, pp. 303, 326-328,344-345,351-353, 363-364.

[21] Gesssner C., Roessler A., Kotttkamp M. (2012), "*UMTS Long Term Evolution (LTE) Technologies Introduction*", Rohde& Schwarz, July, pp. 38-39.

[22] Min S. (2010), "*An Introduction to MIMO Technology*", Advanced Course in Digital Communication,
2007 in Ohtsuki Lab., http://www.sasase.ics.keio.ac.jp/jugyo/2007/MIMO.pdf, May.

[23] Myung H. G. (2008), "*Technical Overview of 3GPP LTE*", May 18,
http://hgmyung.googlepages.com/3gppLTE.pdf, May 2010, pp.39.

[24] Vieira P., Queluz P., Rodrigues A. (2008), "*LTE spectral efficiency using spatial multiplexing MIMO for macro-cells*", IEEE Signal Processing and Communication Systems, 2nd International Conference, pp. 1-6.

[25] Dabrowski J. (2009), "*Radioelectronics*", LiU-Tryck.

[26] Benedetto S. and Biglieri E. (1999), "*Principles of Digital Transmission with Wireless Applications*", Kluwer Academic, Plenum Publishers, New York.

[27] 3GPP TR 36.942(2011), "*Evolved Universal Terrestrial Radio Access (E-UTRA); Radio Frequency (RF) system scenarios*", Version 10.2.0 Release 10, May, pp. 14-15, 98-99.

[28] Ramezani H. (2016), "*MIMO Rayleigh fading Channel Capacity*" Matlab Central,

http://www.mathworks.com/matlabcentral/fileexchange/12491-mimo-rayleigh-fading-channel-capacity.

[29] 3GPP TS 36.306 (2010), "*LTE; Evolved Universal Terrestrial Radio Access (E-UTRA); User Equipment (UE) radio access capabilities*", Version 9.3.0 Release 9, October.

[30] 3GPP TR 25.942(2014), "*Technical Specification Group Radio Access Network; Radio Frequency (RF) system scenarios*", Version 12.0.0 Release 12, September, pp. 26.

[31] 3GPP TR 25.816 (2009), "*Technical Specification Group Radio Access Network; UMTS 900 MHz Work Item Technical Report*", Version 8.0.0 Release 8, September, pp.22.

Online Reference

[1] Pathloss and RSSI Calculator,

http://www.changpuak.ch/electronics/calc_10.php

CURRICULUM VITAE

PERSONAL INFORMATION

Surname, Name: İbişoğlu, İsmail

Date and Place of Birth: 12 August 1989, Trabzon

Marital Status: Single

Email: ismail.ibisoglu@gmail.com

EDUCATION

Degree	Institution	Year of Graduation
B.Sc.	Çankaya Univ., Electronics and Communication Engineering	2013
High School	İncirli High School	2007

WORK EXPERIENCE

Year	Place	Enrollment
08.02.2017- Continue	Vodafone Turkey (Ankara)	Access Network Transport Operation Engineer
15.08.2016- 07.02.2017	Vodafone Turkey (Ankara)	Network (NW) Microwave Operation Engineer
05.01.2016- 12.08.2016	Huawei Turkey (Ankara)	Network Operation Center (NOC) Engineer
18.06.2012 – 13.07.2012	Türk Telekom A.Ş. (General Directorate)	Trainer
15.08.2011 – 16. 09. 2011	Türk Telekom A.Ş. (Ankara Regional Directorate)	Trainer

FOREIN LANGUAGES

Intermediate English, Beginner Spanish

HONOURS

Fall Semester of the 2011-2012 Academic Year Honorary Degree at the Çankaya University

Spring Semester of the 2012-2013 Academic Year Honorary Degree at the Çankaya University

HOBBIES

Books, Music, Football, Basketball and Bowling